Chapter 6

Forced Motions of a Rigid-Body Breakwater

6.1 Introduction

Now the last and most realistic problem will be investigated. This problem treats the breakwater as a rigid body that undergoes periodic wave forcing. This problem is the most realistic because a breakwater truly has physical dimensions in reality and would behave as a rigid body. Furthermore, if a breakwater is in the sea, then it will feel the effects of waves acting on it and not just the effects of its own net buoyancy. It is believed that this model will be a fairly accurate representation of how a breakwater would behave when exposed to the natural ocean environment.

6.2 Equations of Motion

A combination of the equations of motion (EOM's) developed in Chapters 4 and 5 will be used to model the motions of the rigid-body breakwater (RBBW) in this problem. The analytical solution of the EOM's for x and y directions is reviewed in Section 4.2.2; while the analytical solution for the rotations may be seen in Section 5.4 (Equations 5.46, 5.49, 5.52, 5.55, and 5.58).

6.3 Analyzed Cases

These solutions were used and several different cases were analyzed to investigate how varying different parameters affected the motion responses of the breakwater. For this problem, no new parameters were added; just combinations of parameters and initial conditions from previous problems were used. This problem is basically a combination of Chapters 4 and 5. The EOM's and analytical solution from Chapter 4 are combined

with the rotations of the RBBW problem formulation from Chapter 5. The parameters in this problem were varied to see any characteristic responses, and the parameters and initial conditions considered in this problem are summarized in Table 6.1 where $v_x = \dot{x}(0)$, $v_y = \dot{y}(0)$, and $v_\theta = \dot{\theta}(0)$. This table shows the case number, which was used to identify each case analyzed. This number is a series of numbers taken from the parameters and initial conditions. In this problem, the case number uses r, e, a, b, x(0), $\dot{x}(0)$, y(0), $\dot{y}(0)$, θ(0), $\dot{\theta}(0)$ - f_o, ν, Ω in this order to identify the case. For example, the standard case has a case number of 1910001000-559. The standard case will be explained in detail later and is denoted by the shaded cells in Table 6.1. Further, the parameters and initial conditions shown in this table are grouped into series. These groups were used to see how variation of only one parameter would affect the breakwater's response.

6.3.1 Stopping Criteria

During the solution process, some criteria were considered that would cause the solution to stop. These stopping criteria are conditions in which it is felt that the solution should not continue any further. Two of these criteria have already been discussed. The upper boundary restriction of Section 5.2.2.1 actually applies to all of the cases and was discussed in passing in the critical force section of Section 4.4.2. The RBBW has a different upper boundary formulation than the point-mass breakwater (PMBW) case where the PMBW is said to be beyond the upper bound when y>h. The RBBW upper boundary restriction is slightly different because the body is allowed to rotate; thus one side or corner would be out of the region before the center, c, would. Section 5.2.2.2 discusses the rotation restriction, which is more likely and easily achieved in the forced motion case than in the free motion case. This is because the forcing is elliptical in fashion, which can cause the RBBW to rotate with the forcing if the conditions are right and cause the RBBW to rotate excessively. This motion is not desirable since in reality the cables may wrap around the breakwater or become entangled. Therefore, the

restriction of limiting the RBBW to rotations $\pm\pi/2$ or less was imposed. In the solution procedure, if this limit was reached, then the solution would stop and indicate that the initial conditions and parameters were not suitable to keep the rotations to a minimum.

It has been considered that the RBBW will settle to the bottom of the region when two criteria are met. The first criterion is that the normal velocity has become practically zero (i.e., $<1.0\text{x}10^{-6}$). This indicates that the RBBW does not possess enough energy to rebound off of a boundary. The other criterion is that the height of the RBBW is very small (i.e., $< 5.0\text{x}10^{-2}$). These two criteria together work on the premise that the RBBW will settle to the bottom of the region when its height is low and when it does not possess a substantial amount of energy to rebound to a height far above the origin. Also, it is assumed that the force amplitude used is below the critical force, and thus gravity will control and pull the RBBW down. Critical force, for this case, will be explained in Section 6.4.2.

When this situation arises, there is also the possibility that while the RBBW is settling to the bottom, both cables may become taut and the RBBW will start to rock back and forth. In the previous solution, this type of motion is not accounted for, only a situation where one cable becomes taut, and thus the previous solution is no longer valid and this solution is stopped. Therefore, a special formulation was developed to handle this rocking situation and will be discussed in detail in Section 6.5.2.

A similar situation where the previous solution is no longer valid and an alternate solution must be used is where one cable stays taut for a length of time. This situation is thought of as the breakwater sliding along the boundary and occurs when the normal velocity is practically zero and the RBBW is at a height where the breakwater is not considered to settle to the bottom of the region. Sliding occurs in the forcing case because the forcing acts as a elliptical force which is pushing the breakwater one direction and then it reverses and pushes the breakwater in the opposite direction. So, if a

breakwater happens to be near a boundary and is being pushed towards the boundary by the wave forcing, the breakwater may stay on the boundary until the wave forcing reverses direction and stops pushing the breakwater into the boundary. During this time the normal velocity is small, so the breakwater cannot rebound off of the boundary, and the breakwater may slide along the boundary (i.e., the breakwater arcing around the region with a cable being taut). In the previous solution, this type of motion is not accounted for, only a situation where the breakwater is instantaneously on the boundary and thus the previous solution is no longer valid and this solution is stopped. Therefore, a special formulation was developed to handle this sliding situation and will be discussed in detail in Section 6.5.1.

Table 6.1. Parameters and Initial Conditions for Forced Motions of a Rigid-Body Breakwater

Case #														
reabxv$_x$yv$_y$θv$_\theta$-f$_o$vΩ	r	h	e	a	b	x	v$_x$	y	v$_y$	θ	v$_\theta$	f$_o$	ν	Ω
r														
1910001000-359	1.5	1.200	0.9	0.1	0.0	0.0	0.0	0.1	0.0	0.0	0.0	0.3	0.5	0.9
2910001000-359	2.5	2.332	0.9	0.1	0.0	0.0	0.0	0.1	0.0	0.0	0.0	0.3	0.5	0.9
1911001000-359	1.5	1.200	0.9	0.1	0.1	0.0	0.0	0.1	0.0	0.0	0.0	0.3	0.5	0.9
2911001000-359	2.5	2.332	0.9	0.1	0.1	0.0	0.0	0.1	0.0	0.0	0.0	0.3	0.5	0.9
1921001000-359	1.5	1.200	0.9	0.2	0.1	0.0	0.0	0.1	0.0	0.0	0.0	0.3	0.5	0.9
2921001000-359	2.5	2.369	0.9	0.2	0.1	0.0	0.0	0.1	0.0	0.0	0.0	0.3	0.5	0.9
e														
1510001000-359	1.5	1.200	0.5	0.1	0.0	0.0	0.0	0.1	0.0	0.0	0.0	0.3	0.5	0.9
1710001000-359	1.5	1.200	0.7	0.1	0.0	0.0	0.0	0.1	0.0	0.0	0.0	0.3	0.5	0.9
1910001000-359	1.5	1.200	0.9	0.1	0.0	0.0	0.0	0.1	0.0	0.0	0.0	0.3	0.5	0.9
1110001000-359	1.5	1.200	1.0	0.1	0.0	0.0	0.0	0.1	0.0	0.0	0.0	0.3	0.5	0.9
b=0 (circle)														
1910001000-359	1.5	1.200	0.9	0.1	0.0	0.0	0.0	0.1	0.0	0.0	0.0	0.3	0.5	0.9
1920001000-359	1.5	1.269	0.9	0.2	0.0	0.0	0.0	0.1	0.0	0.0	0.0	0.3	0.5	0.9
1930001000-359	1.5	1.327	0.9	0.3	0.0	0.0	0.0	0.1	0.0	0.0	0.0	0.3	0.5	0.9
a=b (square)														
1911001000-359	1.5	1.200	0.9	0.1	0.1	0.0	0.0	0.1	0.0	0.0	0.0	0.5	0.5	0.9
1922001000-359	1.5	1.269	0.9	0.2	0.2	0.0	0.0	0.1	0.0	0.0	0.0	0.5	0.5	0.9
1933001000-359	1.5	1.327	0.9	0.3	0.3	0.0	0.0	0.1	0.0	0.0	0.0	0.5	0.5	0.9
a>b (rectangle)														
1911001000-359	1.5	1.200	0.9	0.1	0.1	0.0	0.0	0.1	0.0	0.0	0.0	0.5	0.5	0.9
1921001000-359	1.5	1.269	0.9	0.2	0.1	0.0	0.0	0.1	0.0	0.0	0.0	0.5	0.5	0.9
1931001000-359	1.5	1.327	0.9	0.3	0.1	0.0	0.0	0.1	0.0	0.0	0.0	0.5	0.5	0.9
f$_o$														
1910001000-159	1.5	1.200	0.9	0.1	0.0	0.0	0.0	0.1	0.0	0.0	0.0	0.1	0.5	0.9
1910001000-259	1.5	1.200	0.9	0.1	0.0	0.0	0.0	0.1	0.0	0.0	0.0	0.2	0.5	0.9
1910001000-359	1.5	1.200	0.9	0.1	0.0	0.0	0.0	0.1	0.0	0.0	0.0	0.3	0.5	0.9
1910001000-459	1.5	1.200	0.9	0.1	0.0	0.0	0.0	0.1	0.0	0.0	0.0	0.4	0.5	0.9
1910001000-559	1.5	1.200	0.9	0.1	0.0	0.0	0.0	0.1	0.0	0.0	0.0	0.5	0.5	0.9
Ω														
1910001000-355	1.5	1.200	0.9	0.1	0.0	0.0	0.0	0.1	0.0	0.0	0.0	0.3	0.5	0.5
1910001000-3575	1.5	1.200	0.9	0.1	0.0	0.0	0.0	0.1	0.0	0.0	0.0	0.3	0.5	0.75
1910001000-359	1.5	1.200	0.9	0.1	0.0	0.0	0.0	0.1	0.0	0.0	0.0	0.3	0.5	0.9
1910001000-3515	1.5	2.332	0.9	0.1	0.0	0.0	0.0	0.1	0.0	0.0	0.0	0.3	0.5	1.5
1910001000-3520	1.5	1.200	0.9	0.1	0.0	0.0	0.0	0.1	0.0	0.0	0.0	0.3	0.5	2.0

6.3.2 Standard Case

A standard case was developed for this problem as a starting point for the variation of parameters and initial conditions. The standard parameters and initial conditions for this RBBW problem under wave forcing are:

$$
\begin{array}{lll}
r=1.5 & e=0.9 & \\
a=0.1 & b=0.0 & \\
x(0)=0.0 & y(0)=0.1 & \theta(0)=0.0 \\
\dot{x}(0)=0.0 & \dot{y}(0)=0.0 & \dot{\theta}(0)=0.0 \\
f_o=0.3 & \nu=0.5 & \Omega=0.9
\end{array}
\qquad (6.1)
$$

As seen above in the standard initial conditions, the RBBW is started from a similar position as in the PMBW problem undergoing forced wave motions. Again, this position was chosen because it was felt to be more realistic to the true behavior of a breakwater. Further, the RBBW is started with no initial rotation or rotational velocity because in this forced motion case it is felt that the restriction of $\theta \leq \pi/2$ might be violated if it were given initial rotational energy. The standard forcing parameters were kept the same as in the PMBW case except f_o. The forcing amplitude, f_o, of 0.5 used in the PMBW forced motion case was found to be greater than the critical force using the standard conditions for the RBBW case. Thus, as seen in Equation 6.1, the standard forcing amplitude used for the RBBW under forcing will be 0.3. The critical force for this problem will be discussed in detail in Section 6.4.2. Once the values were selected through judgement and experience, the parameters and initial conditions were varied about the standard case to see any characteristic response behavior to the varying of the values.

6.4 Analysis of Data

Cases were analyzed and data was collected to see what types of characteristic behavior the RBBW exhibited under forced motions. Again, several types of graphs were used to evaluate the responses of the RBBW, including rotation vs. time plots. With forcing now involved in the analysis, special attention must be paid to the fact that the RBBW might

start to slide along the boundary or rock at the bottom of the region, as discussed previously. Also, the stopping criteria discussed in Section 6.3.1 must be considered.

6.4.1 Observations

The radius (i.e., the length of the cables) was the first parameter varied to see how the RBBW under forced wave motions would respond. Similar to the other problems investigated, there does not appear to be a significant characteristic differences between the motions of a case that has a radius of 1.5 and a case that has a radius of 2.5. However, there are two notable differences between the two radii. First, the cases with a radius of 1.5 have a sharper point at the bottom than those of the 2.5 radius case, which is shallower and leads to a flatter pattern of motion at the bottom of the region, as discussed previously in Chapter 5. Figures 6.1 and 6.2 illustrate the difference in size and range of motions of the center of the RBBW, dependent upon the mooring cable radius. However, the motion in the graph of the 2.5 radius case is not complete, because of the second noticeable difference in the two radii. The 2.5 radius case reaches a rotation value of $\pi/2$ before the motion settles to the bottom of the region as in the 1.5 radius case. All other parameters and initial conditions were kept the same for both cases. This excessive rotation indicates that the 2.5 case has a forcing amplitude greater than that of the critical force. The critical force for these two cases will be discussed in more detail in Section 6.4.2. Though this occurs, the characteristic nature of motions produced by the two radii may still be seen.

The same response of a flatter region may also be seen in the varying of the dimensions a and b. As the dimensions increase, it may be seen that the bottom of the region becomes flatter. This flatness is further exaggerated by the increase of the radius (Figs. 6.3–6.6). Note that Figs. 6.1-6.6 are all plotted to the same scale for comparison purposes. Figure 6.6, however, has some data cut off because of its large motions. Figure 6.7 shows the full range of motions for the case in Fig. 6.6 but plotted at a scale twice as big as the scale of Figs. 6.1-6.6. Also, by looking back at Fig. 5.1, it may be seen that as the distance

between the connection points, V and W, is increased, the flatter the bottom of the region becomes. Further, the smaller the dimensions, the greater the rotations. In other words, as the size of the breakwater increases, there is less potential to rotate. This is because if the moment of inertia is less, the resistance to rotation is less and the RBBW rotates more. Figures 6.8 through 6.10 show that when the dimension a is increased for a rectangular section from 0.1 to 0.2 to 0.3 with b=0.1, the magnitude and amount of rotation are increased but the frequency of large swings in the rotation decreases. What is meant by large swings in the rotation is that say the RBBW has a large value of θ (i.e., near $+\pi/2$) and then a short time later, has a small value of θ (i.e., near $-\pi/2$). This large difference in rotation in a short period of time would consume more of the energy of the breakwater than would several smaller swings in rotation. Further, larger dimensions give a larger moment of inertia and hence rotation is being resisted more and the large swings in the amount of rotation are decreased. Notice that as the graphs reach the end, the magnitudes of the rotations get smaller and the frequency increases, indicating that the breakwater is possibly approaching a rocking condition, discussed in Section 6.5.2. Numerically, the dimensional values with the associated nondimensional mass moments of inertia for the various shapes may be seen in Table 5.2.

Fig. 6.1. y vs. x, Case 1910001000-359 (r=1.5, a=0.1, b=0.0)

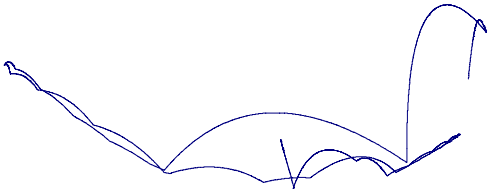

Fig. 6.2. y vs. x, Case 2910001000-359 (r=2.5, a=0.1, b=0.0)

Fig. 6.3. y vs. x, Case 1911001000-359 (r=1.5, a=0.1, b=0.1)

Fig. 6.4. y vs. x, Case 2911001000-359 (r=2.5, a=0.1, b=0.1)

Fig. 6.5. y vs. x, Case 1921001000-359 (r=1.5, a=0.2, b=0.1)

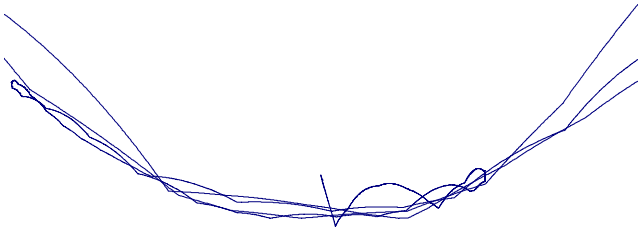

Fig. 6.6. y vs. x, Case 2921001000-359 (r=2.5, a=0.2, b=0.1)

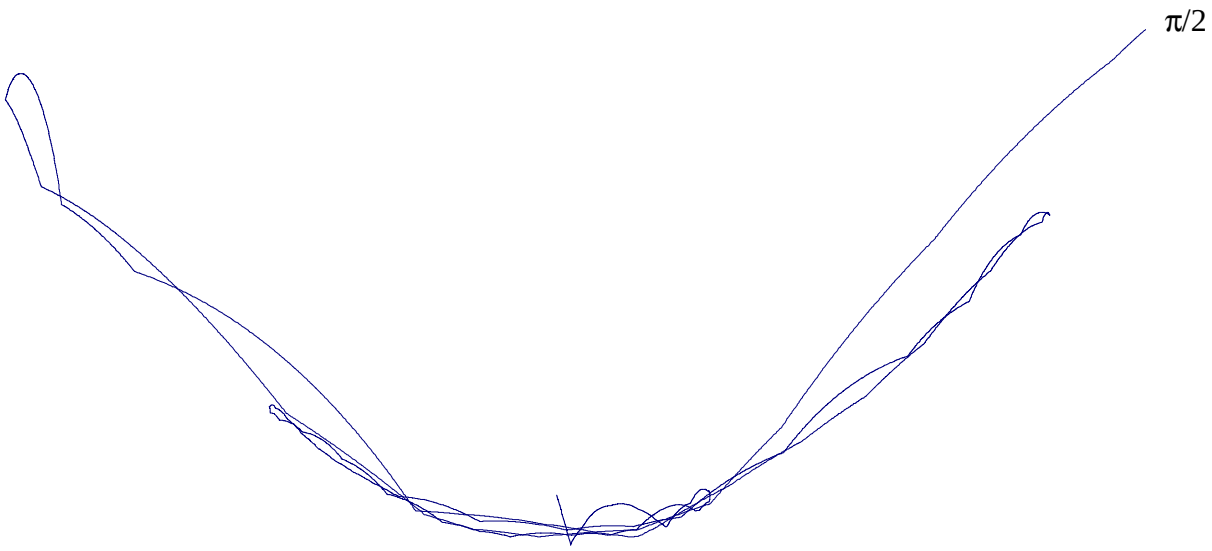

Fig. 6.7. y vs. x, 2921001000-359
(r=2.5, a=0.2, b=0.1)
(twice scale)

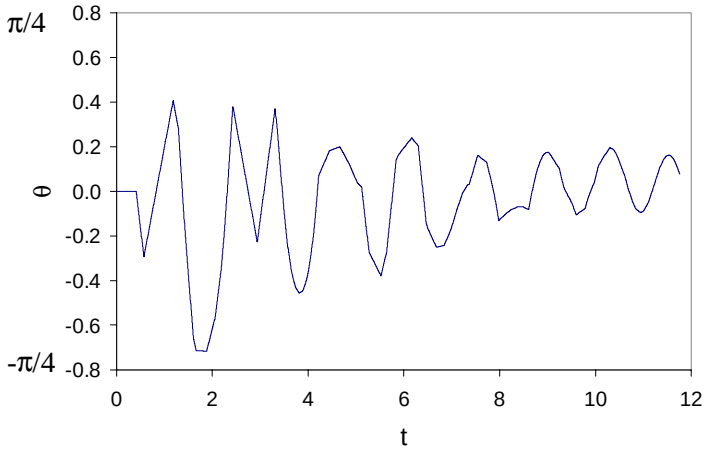

Fig. 6.8. θ vs. t, Case 1911001000-359
(a=0.1, b=0.1)

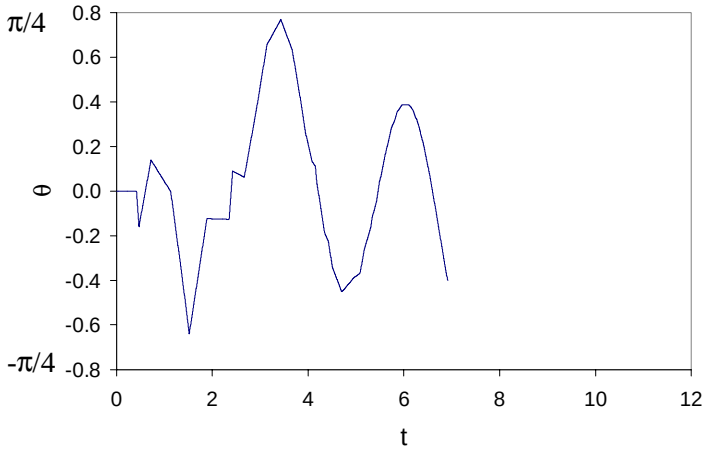

Fig. 6.9. θ vs. t, Case 1921001000-359
(a=0.2, b=0.1)

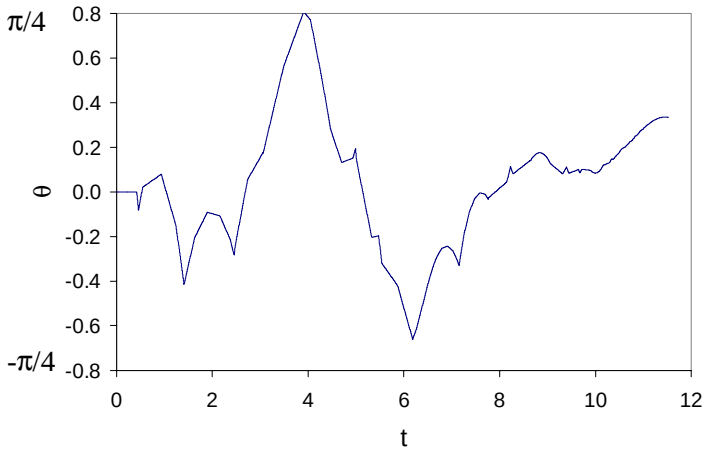

Fig. 6.10. θ vs. t, Case 1931001000-359
(a=0.3, b=0.1)

The variation of the coefficient of restitution, e, in this problem does not produce any noticeable characteristic differences from the characteristics previously discussed. As the coefficient of restitution was varied from 1.0 to 0.9 to 0.7 and to 0.5, the motions of the RBBW became less active as more energy was dissipated through the impacts occurring as the cables became taut. This behavior is illustrated in Figs. 6.11-6.14 where the corresponding v_n^- vs. t plots show that the energy tends to decrease if e<1. The time scale in Fig. 6.11 is different than in Figs. 6.12-6.14. The chaotic nature of the case where e=1.0 may be attributed to the forcing adding energy to the system while gravity tries to draw the RBBW downward. One point which should be noted is that during the solution of the e=1.0 case, the rotation of the RBBW surpasses the $\pi/2$ restriction and the solution is stopped. The trajectory plot of this case may be seen in Fig. 6.15. Further, Fig. 6.16 shows the rotation versus time plot for this case where the limit of $\pi/2$ is indicated. This excessive rotation may be attributed to the fact that no energy is lost at the various impacts, and thus the motions are not damped out and excessive rotations become likely. As e is decreased, more and more energy is lost from the system, causing the RBBW to move less around the region and experience lower snap loading. As time goes on, more energy is dissipated and gravity starts to control the motions of the breakwater and draws it down to the equilibrium state at the bottom of the region. Thus, the lower the e value, the less time the breakwater will move around the region before it settles to the bottom of the region because of its loss of energy and the influence of gravity.

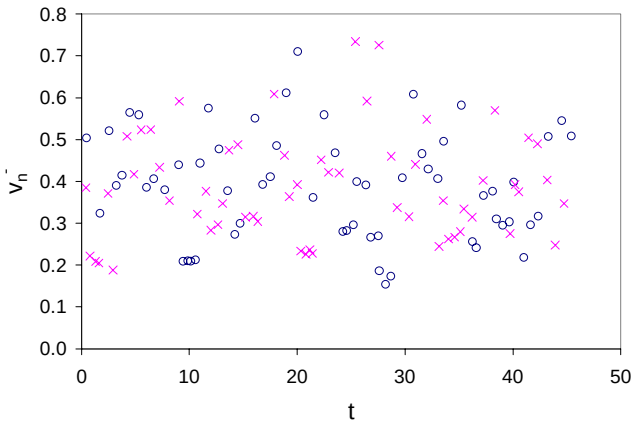

Fig. 6.11. v_n^- vs. t, Case 1110001000-359 (e=1.0)

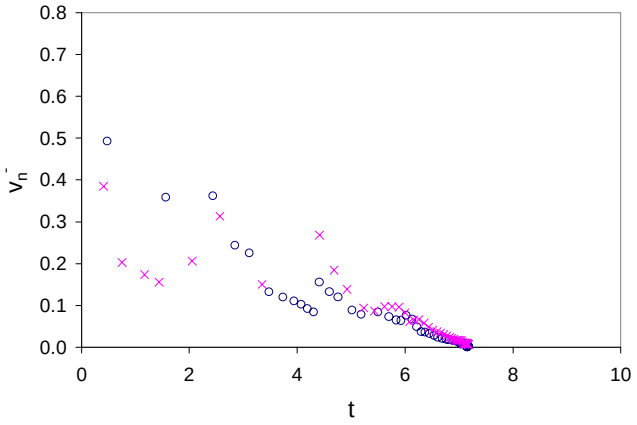

Fig. 6.12. v_n^- vs. t, Case 1910001000-359 (e=0.9)

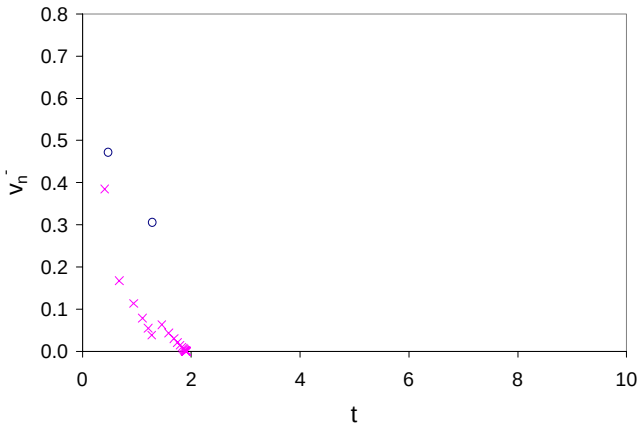

Fig. 6.13. v_n^- vs. t, Case 1710001000-359 (e=0.7)

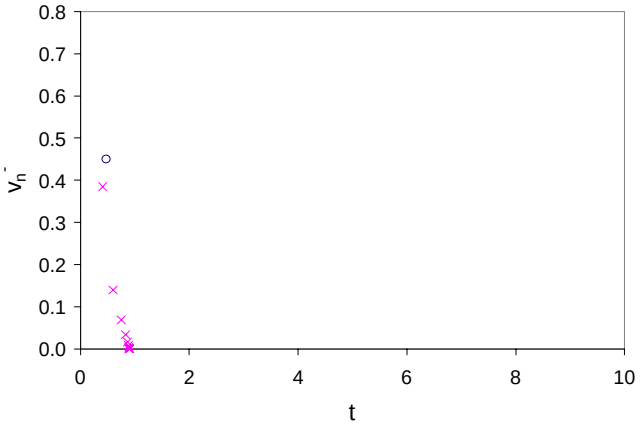

Fig. 6.14. v_n^- vs. t, Case 1510001000-359 (e=0.5)

Fig. 6.15. y vs. x, Case 1110001000-359 (e=1.0)

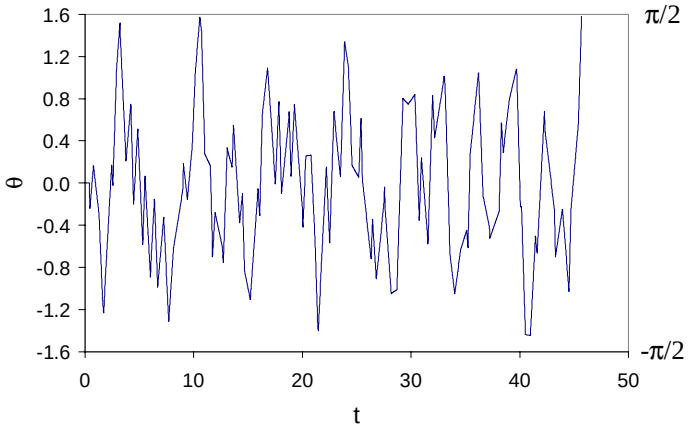

Fig. 6.16. θ vs. t, Case 1110001000-359 (e=1.0)

As the force amplitude, f_o, was increased in steps of 0.1, it was seen that the rotation limit of $\pi/2$ was first reached when $f_o=0.5$. However, when a smaller step of 0.01 in the variation of the force amplitude was used, it was found that the rotation limit was reached at 0.31. This force amplitude was found to be the critical force, which will be discussed in more detail in Section 6.4.2. The cases seen in Table 6.1 that have f_o less than 0.5 settle to the bottom of the region. This would indicate that these values are below the critical force, but this is not true since the critical force here is the first force which causes the breakwater to rotate past the rotation limit of $\pm\pi/2$. These cases settle to the bottom because it is possible for a case with a forcing amplitude greater than that of the critical force to have gravity control even though the rotation limit was reached at a lower forcing amplitude. This phenomenon is due to the many variables and degrees of freedom involved in the nonlinear solutions. This is why a detailed analysis of the critical force was performed.

The forcing parameter Ω was varied to see its effect on the response of the RBBW under forced motions. The cases analyzed in this section used the standard case parameters and initial conditions expect that the value of Ω was varied from 0.5 to 0.75 to 0.9 to 1.5 to 2.0 to produce the data. No noticeable characteristic features appear in the trajectory plots, and they will not be shown. Figures 6.17-6.21 show the plots of θ vs. t for these cases. In these plots it also appears that as the value of Ω is increased, the magnitude of the rotations also increases though nonlinearly. The rotations increase until the rotation limit is exceeded, which occurs in the $\Omega=2.0$ case, seen in Fig. 6.21. The v_n^- vs. time plots, seen in Figs. 6.22-6.26, also shows some interesting phenomena. One interesting feature is seen in Figs. 6.22, 6.24, and 6.26 where there are segments of only x's or only o's close to each other. By looking at the trajectory and impact data, it can be deduced that this is caused by the RBBW bouncing down a boundary for a while.

As seen in the various normal velocity just before impact versus time (v_n^- vs. t) plots throughout this chapter, patterns of x's and o's may be noticed which are similar to

patterns previously seen in other problems. This problem appears to have all of the characteristic patterns discussed in earlier problems. Some of the plots have the normal velocities consistently higher on one boundary than the other, as seen in Fig. 6.22. This may indicate that the RBBW is grazing off one boundary with little normal velocity, and striking the other boundary more directly and producing a larger normal velocity before impact. Another pattern shows the normal velocities of the two boundaries converging and then diverging, like a serpentine pattern, as seen in Fig. 6.25. A similar pattern is seen where the normal velocities of the two boundaries intertwine in and out of each other similar to braiding. This may be seen in Figs. 6.23 and 6.24. These patterns are most likely due to the elliptical forcing which is continually changing direction. For example, say the RBBW is headed towards the right boundary and the forcing is acting in the same direction; then the normal velocity will be high at impact. Then after the rebound the RBBW is headed towards the left boundary but the forcing is acting in the opposite direction; then the normal velocity will be low when it strikes the left boundary, showing up on the graph as a separation in the braids. If both boundaries are struck in succession with similar conditions and the forcing has switched direction, then the normal velocities may have the same value, indicated on the v_n^- vs. t graph as a point of convergence or overlapping.

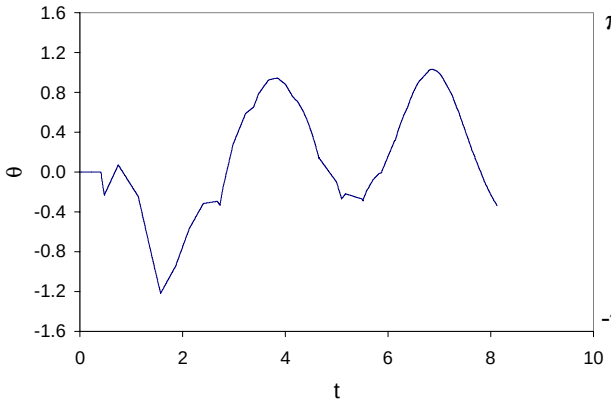

Fig. 6.17. θ vs. t, Case 191001000-355 (Ω=0.5)

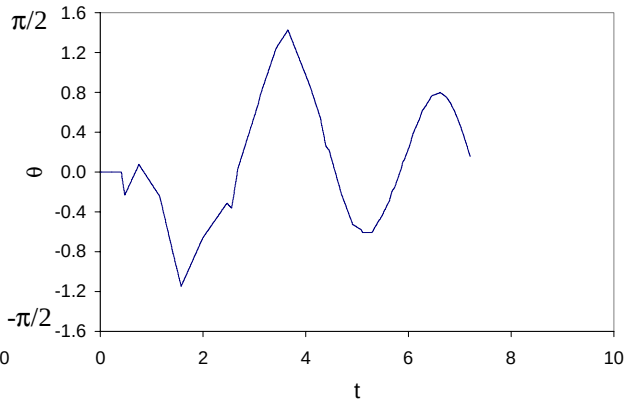

Fig. 6.18. θ vs. t, Case 191001000-3575 (Ω=0.75)

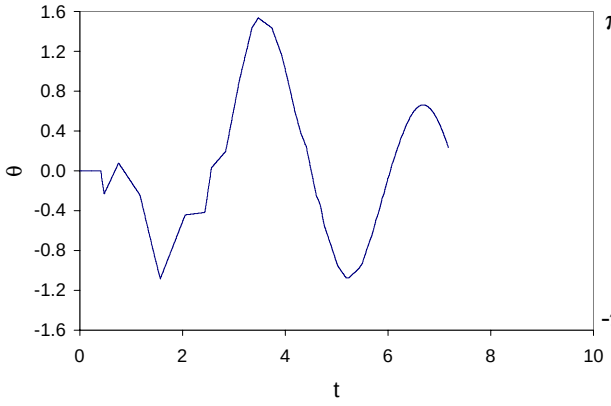

Fig. 6.19. θ vs. t, Case 1910001000-359 (Ω=0.9)

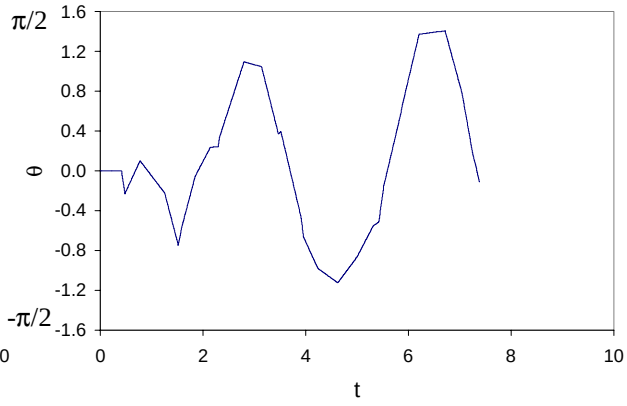

Fig. 6.20. θ vs. t, Case 1910001000-3515 (Ω=1.5)

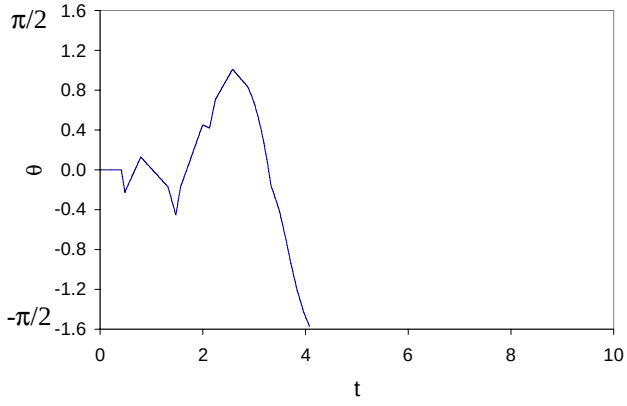

Fig. 6.21. θ vs. t, Case 1910001000-3520 (Ω=2.0)

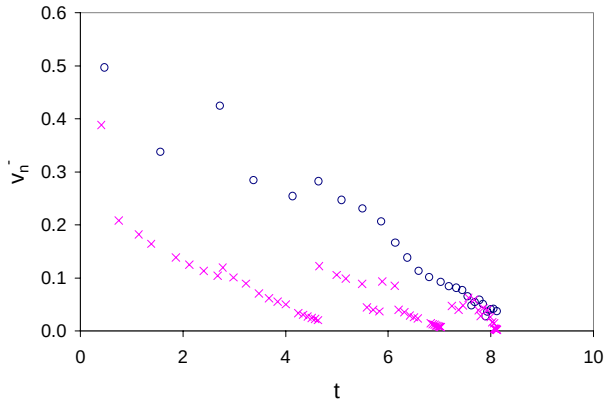

Fig. 6.22. v_n^- vs. t, Case 1910001000-355 (Ω=0.5)

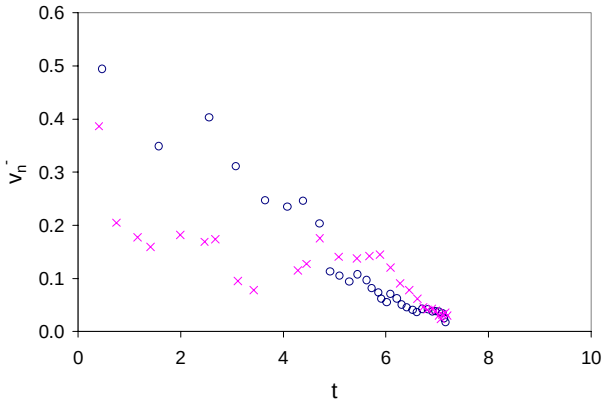

Fig. 6.23. v_n^- vs. t, Case 1910001000-3575 (Ω=0.75)

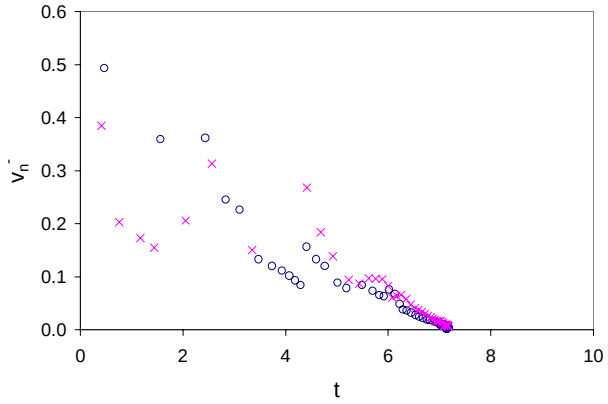

Fig. 6.24. v_n^- vs. t, Case 1910001000-359 (Ω=0.9)

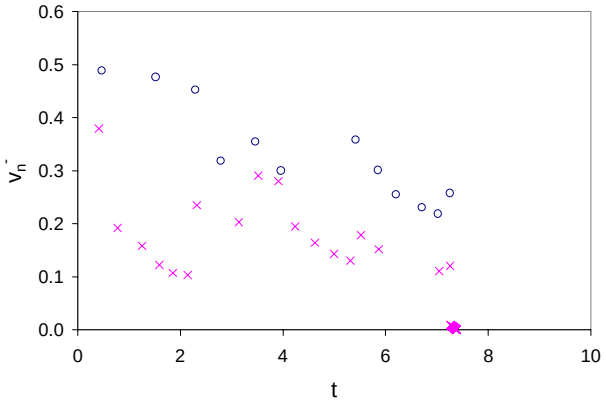

Fig. 6.25. v_n^- vs. t, Case 1910001000-3515 (Ω=1.5)

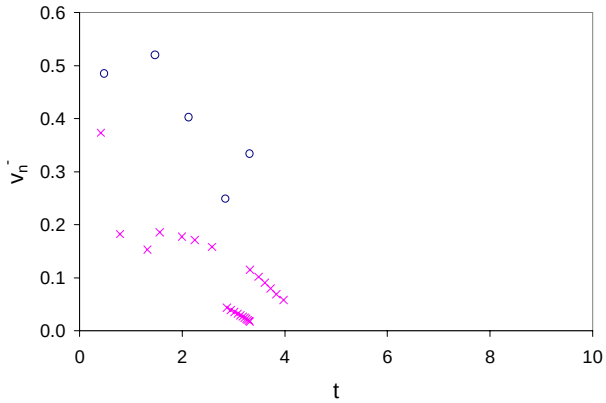

Fig. 6.26. v_n^- vs. t, Case 191001000-3520 (Ω=2.0)

6.4.2 Critical Force

The critical force was investigated in this problem and is similar in concept to that discussed previously in Section 4.4.2. The critical force was originally defined as the forcing amplitude, f_o, which would cause the breakwater to hit the upper boundary (y=h), which indicates that the forcing was so large that it controlled the motions of the breakwater and caused it to hit the sea floor. Now that a more accurate and sensitive model is being investigated, this definition must be slightly modified. For the rigid-body analysis, the critical force turned out to be the force that causes the breakwater to rotate past $\pm\pi/2$. This limit was reached before the y=h limit because of the sensitivity of the RBBW to rotations. This limit is significant because if the breakwater rotates past this value the mooring lines may become entangled, which is undesirable.

Two critical force cases were investigated in depth for this problem, where plots of f_{cr} vs. e and Ω were produced for both. Both analyses were performed with the circular shape of the standard case; however, two values of the length of the mooring lines, r=1.5 and 2.5, were used to see the effect on the critical force. These investigations were performed by fixing all of the case conditions and increasing f_o until θ reached the limit of $\pm\pi/2$. The critical force for some other cases, where the size of the RBBW was varied, were determined under standard parameters (i.e., e=0.9 and Ω=0.9) to see what influence the size and shape of the breakwater has on the critical force.

Critical force results when varying the size of the RBBW with respect to the standard parameters and initial conditions may be seen in Table 6.2. It can be seen from the results summarized in this table that typically as the size of the RBBW is increased, as well as the mass moment of inertia, the higher the force amplitude has to be in order to cause the RBBW to rotate past the rotation limit. The exceptions to this conclusion, seen in the table, are most likely due to the fact that the problem being investigated is highly

nonlinear in nature from the many variables involved in the solution. Thus, one small change in the variables may cause a significant change in the results. The critical forces for the r=2.5 cases tend to be less than the critical forces for the r=1.5 cases. Again, this is most likely due to the larger area and flatter boundaries of the r=2.5 cases. Another difference is seen between the circular and square or rectangular shapes. The circular shapes have lower critical forces than the square or rectangular shapes. The differences between the critical force of these different shapes may be due to the fact that the connection points are at different locations (Figs. 5.2a-c).

Table 6.2 Critical Force Results of Different Size RBBW's with Different r Values and Same Standard Conditions

r=1.5	a	b	f_{cr}	r=2.5	a	b	f_{cr}
circle	0.1	0	0.31	**circle**	0.1	0	0.10
	0.2	0	0.42		0.2	0	0.18
	0.3	0	0.40		0.3	0	0.30
square	0.1	0.1	0.32	**square**	0.1	0.1	0.28
	0.2	0.2	0.34		0.2	0.2	0.33
	0.3	0.3	0.60		0.3	0.3	0.35
rectangle	0.2	0.1	0.68	**rectangle**	0.2	0.1	0.27
	0.3	0.1	0.67		0.3	0.1	0.35

Plots of the critical force versus the coefficient of restitution, e, and the wave frequency, Ω, were created (Figs. 6.27, 6.28, 6.29, and 6.30). These plots for the two different mooring line lengths were produced by fixing all of the standard case conditions (e.g., a=0.1, b=0.0) except either e (Figs. 6.27, 6.29) or Ω (Figs. 6.28, 6.30) was chosen, and f_o was increased until the calculated θ value reached the rotation angle of $\pm\pi/2$. For the value of r=1.5 it is seen in Figs. 6.27 and 6.28 that the critical force for the standard case (e=0.9, Ω=0.9) is around 0.31. This means that when $f_o=0.31=f_{cr}$ for the standard case conditions, the RBBW will rotate to an angle of $\pm\pi/2$ sometime during its motions. This is why a force amplitude of 0.3 was used as the standard amplitude, because any f_o above 0.31 is above the critical force and the RBBW may rotate past the rotation restriction. In the r=2.5 analysis, it may be seen in Figs. 6.29 and 6.30 that the critical force for the

given conditions is around 0.10. This means that when $f_o=0.10=f_{cr}$ for the conditions, the RBBW will rotate to an angle of $\pm\pi/2$. This is why when the force amplitude of 0.3 was used during the analysis of the case in Table 6.1, the RBBW rotated past the rotation restriction, because $f_o>f_{cr}$. The critical force decreased from 0.31 in the r=1.5 case to a value of 0.10 as the size of the region increased. This is because there is more area for the breakwater to move around and more possibility for the breakwater to rotate excessively.

Further, Figs. 6.27-6.29 show a decreasing nature of the critical force as the variables e and Ω increase. However, Fig. 6.30 shows that the value of f_{cr} is basically increasing with Ω. This may be attributed to the fact that the r=2.5 region is larger and as the frequency increases the RBBW may be pushed around more rather than impacting a boundary which typically causes the breakwater to rotate excessively. It is also seen that the critical force plots are not monotonic in nature; they contain some local maxima and minima, and thus special attention must be paid to the critical force for the situation being investigated.

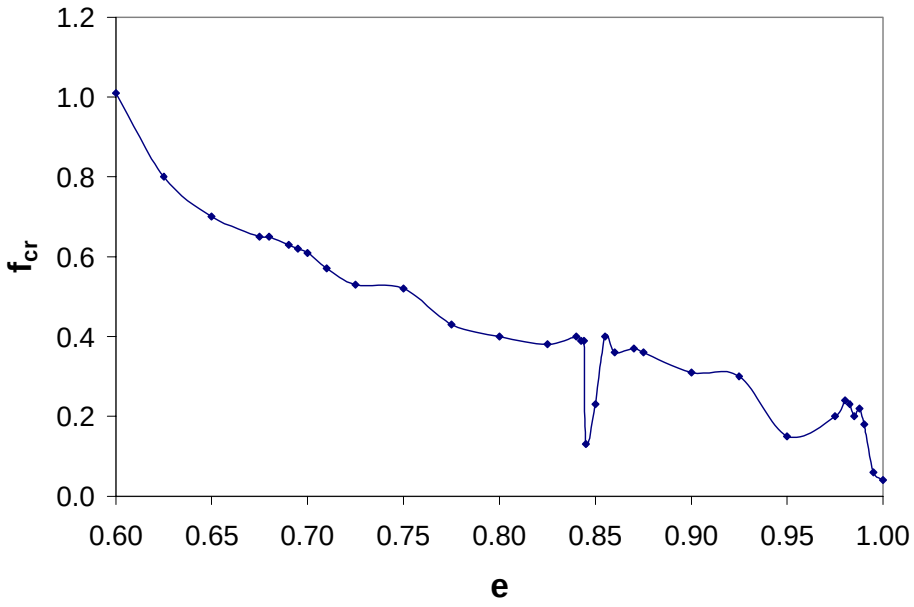

Fig. 6.27. Critical Force vs. e (r=1.5)

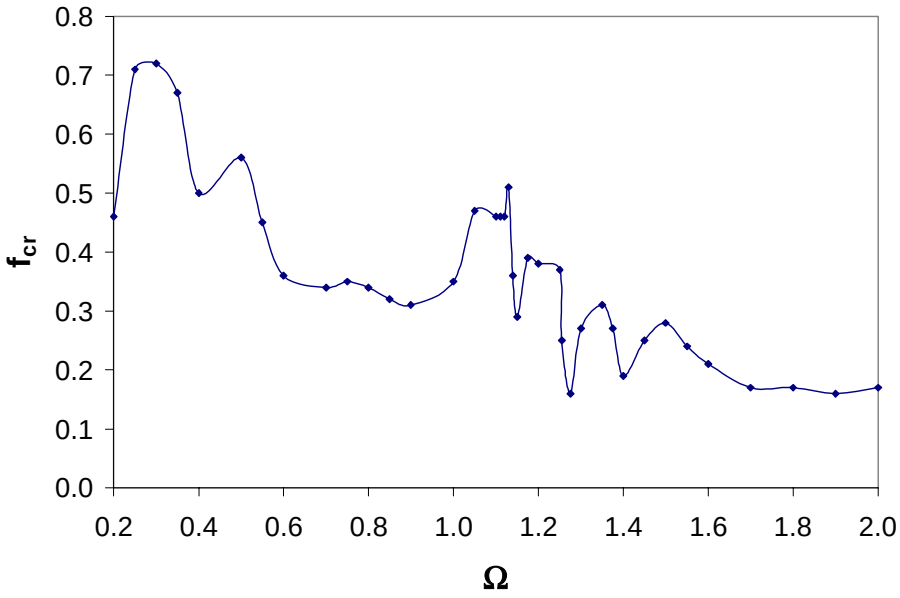

Fig. 6.28. Critical Force vs. Ω (r=1.5)

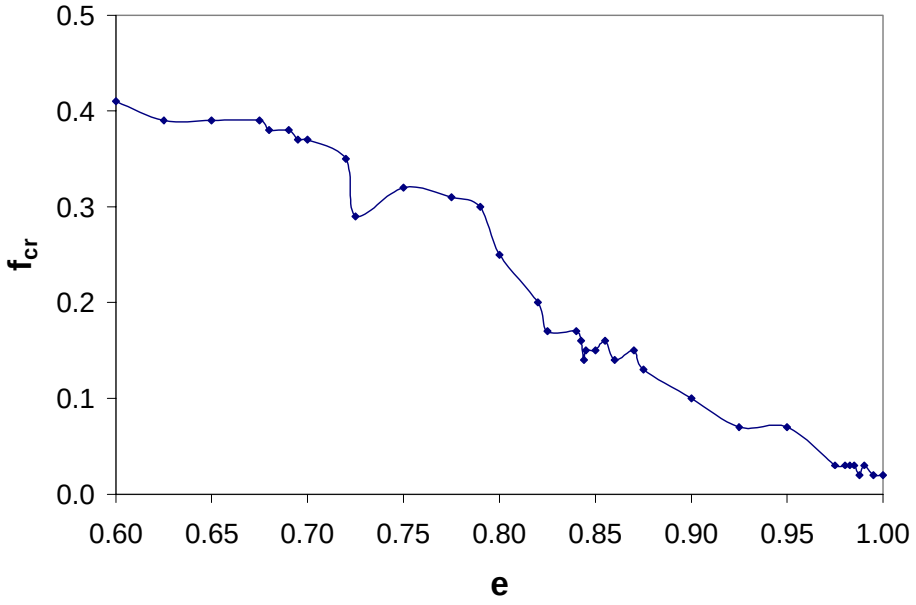

Fig. 6.29. Critical Force vs. e (r=2.5)

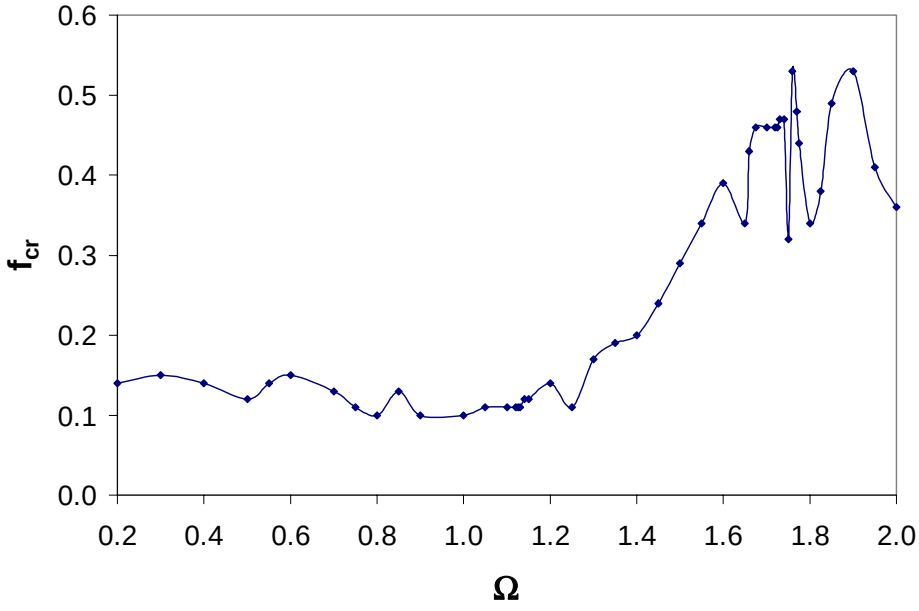

Fig. 6.30. Critical Force vs. Ω (r=2.5)

6.4.3 Norms

The norm plots created for this problem were done so with a set of given data for two cases where r=1.5 and r=2.5. Norms for this problem are either maximum data points or summation of data. Five norms were investigated in this problem; three dealt with the normal velocity just before impact, v_n^-, as follows:

$$\rho_1 = \max_t(v_n^-) \tag{6.2}$$

$$\rho_2 = \sum_{t=0}^{10} v_n^- \tag{6.3}$$

$$\rho_3 = \sum_{t=0}^{\infty} v_n^- \tag{6.4}$$

The other two dealt with the maximum height, y_{max}, and rotation, θ_{max}, which the RBBW attained during its period of motion. The data used in the determination of the norms was the same data used to produce the trajectory and normal velocity vs. time plots. The norms are plotted versus the magnitude of the forcing, f_o, for a given set of parameters in Figs. 6.31-6.38. The standard case parameters and initial conditions (Equation 6.1) were used to create these plots with the exception of the f_o parameter which was varied to the value of the critical force for that case. Figures 6.31-6.34 are the norm plots for the r=1.5 case while Figs. 6.35-6.38 are the norm plots for the r=2.5 case.

As seen in Figs. 6.31 and 6.35, the phenomenon of a critical forcing is reinforced. It can be seen that as the forcing is increased, $|\theta|_{max}$ increases to the rotation limit of $\pi/2$, and the corresponding force amplitude is at the predetermined value of f_{cr}. When the forcing is low, the initial height of y_o=0.1 is y_{max} (Figs. 6.32 and 6.36). This is due to gravity controlling the motions at this low forcing. As the forcing increases, the response becomes more and more controlled by the forcing and the maximum height attained by the RBBW may increase. However, in the r=2.5 case, y_{max} never gets above the initial height before the rotation restriction is reached. This is most likely due to the fact that

the bottom of the r=2.5 region is flatter than that of the r=1.5 case, thus there is more area for the breakwater to travel about and more possibility for it to rotate excessively.

As the force amplitude, f_o, is increased, the ρ_1 norms (Figs. 6.33 and 6.37) tend to stay constant. This is different than the behavior seen in the PMBW under forcing (Section 4.4.3) where the value of ρ_1 increased as the force amplitude increased. The norm ρ_1 may have kept a constant value in this problem because of the rotations being introduced into the RBBW response at the time of impact (Equations 5.69, 5.70, 5.97, and 5.98). More likely, though, as seen in Equation 6.2, this norm is the greatest normal velocity value throughout the motions of the RBBW and the normal velocity is usually at a maximum around the first impact, as can be seen in Figs. 6.22-6.26. However, in the RBBW case the breakwater has dimensions unlike the PMBW case, and thus the RBBW is closer to the boundaries even when started from the same initial position because of these dimensions. As the forcing increases, the PMBW travels a farther distance than the RBBW does to hit a boundary for the first impact. Therefore, the PMBW will gain more velocity from the wave forcing than the RBBW would because it travels farther. Thus, it may be concluded that the norm ρ_1 may stay constant in the RBBW case because of its rotations and dimensions.

The cumulative norms ρ_2 and ρ_3 (Figs. 6.33, 6.34, 6.37, and 6.38) exhibit some interesting behavior. In the r=1.5 analysis, ρ_2 and ρ_3 appear to stay constant at lower values of f_o and decrease while acting erratically at higher values of f_o (Figs. 6.33 and 6.34). By examining the θ vs. time plots for the cases used to produce these norms, it was found that the magnitude and frequency of jumping or swinging between extreme values stay low and constant at low values of f_o and then increase at higher values of f_o. This increase in rotational movement would transform some of the translational energy into rotational energy, and thus decrease the velocity with which a boundary is hit. Therefore, as the value of f_o increases, the magnitude of rotations increases (Fig. 6.31)

which causes large swings in θ over time, and the impact energy which is derived from the velocities of the breakwater is reduced; this is reflected in the ρ_2 and ρ_3 plots.

In the r=2.5 analysis, ρ_2 and ρ_3 appear to decrease as the value of f_o increases and then appear to increase and then decrease again while acting erratically at higher values of f_o (Figs. 6.37 and 6.38). The same rotation phenomenon is exhibited here; however, in this case, the swings in rotation extremes increase and then start decreasing and increase again, giving the dipping nature seen in Figs. 6.37 and 6.38. The interesting behavior seen in these plots indicates that there may be some optimum value of wave forcing amplitude for these cases where the wave energy may be dissipated most effectively. But the unpredictable and erratic response seen in these norm plots may only be explained and most likely attributed to the highly nonlinear nature of the problem. An increase in the forcing amplitude, f_o, does not necessarily cause the norms to increase in a nice geometric pattern.

In Figs. 6.33 and 6.34 and also in Figs. 6.37 and 6.38, it may be noticed that the plots of ρ_2 and ρ_3 are similar because the data are almost equal for both sets of norms. They stay the same because the time, t, does not get above t=10 in most cases before the RBBW settles to the bottom. The limit of t=10 for ρ_2 comes from Equation 6.3. This phenomenon indicates that the RBBW dissipates wave energy within a short period. However, it reaches a critical force at a lower force than the PMBW. This is because the critical forces are defined in different manners and the RBBW is more sensitive to its critical force definition than the PMBW. A true comparison of the PMBW case with the RBBW can not be made since the PMBW is infinitesimally small with no rotations and the RBBW has a shape and the ability to rotate. Therefore, because these are differences between the two models, a direct comparison can not be made because the proportional effects of the differences are not known.

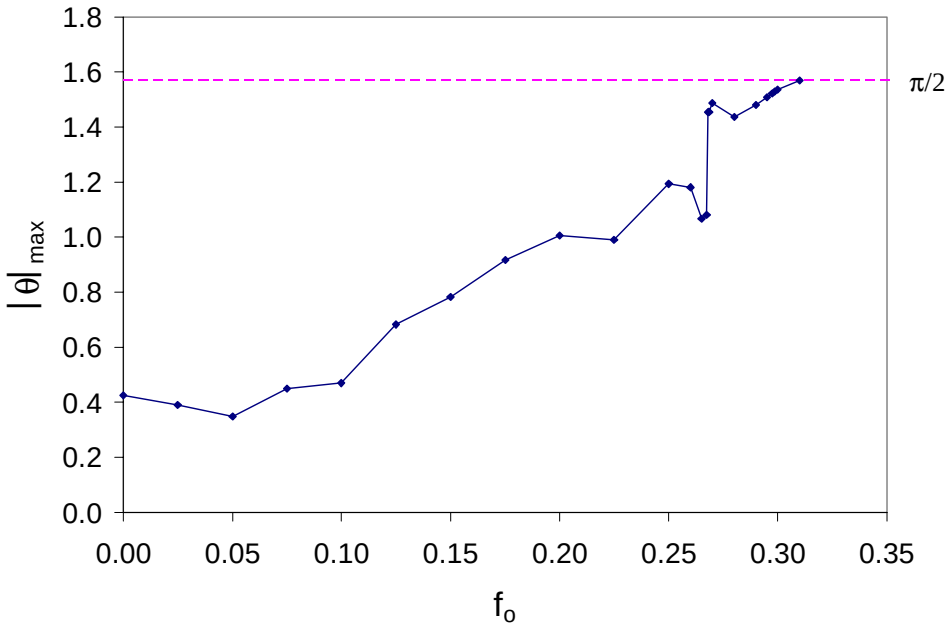

Fig. 6.31. $|\theta|_{max}$ vs. f_o, Norm Plot (r=1.5)

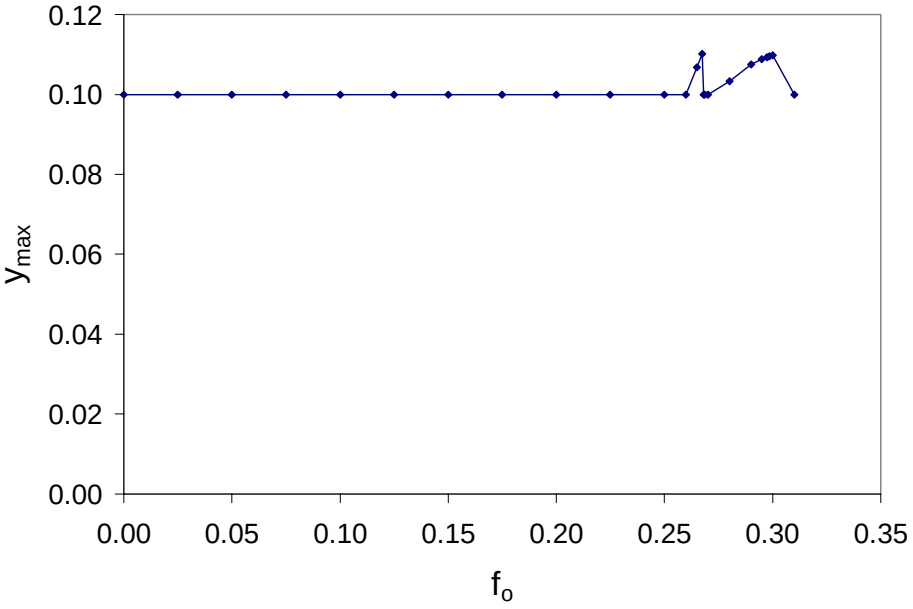

Fig. 6.32. y_{max} vs. f_o, Norm Plot (r=1.5)

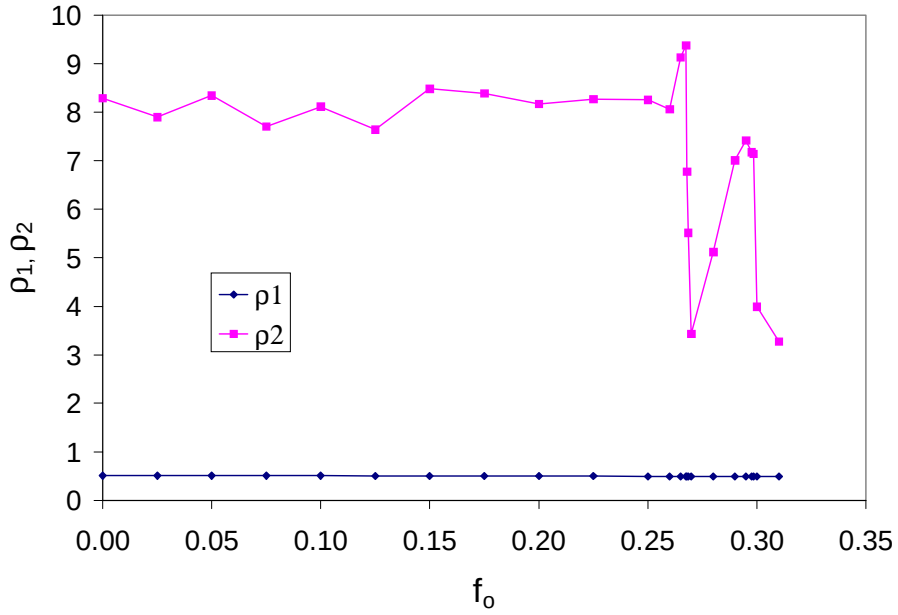

Fig. 6.33. ρ_1 and ρ_2 vs. f_o, Norm Plot (r=1.5)

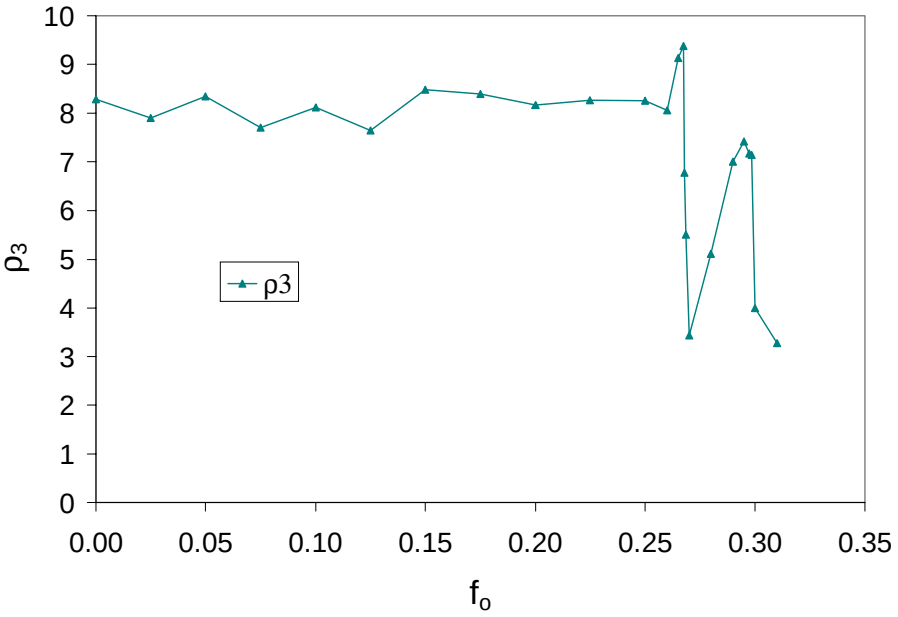

Fig. 6.34. ρ_3 vs. f_o, Norm Plot (r=1.5)

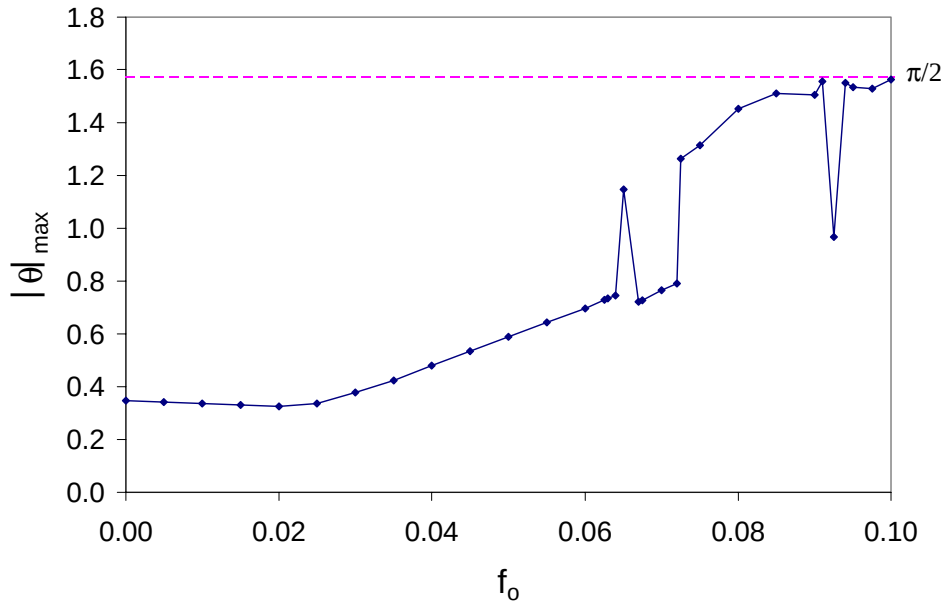

Fig. 6.35. $|\theta|_{max}$ vs. f_o, Norm Plot (r=2.5)

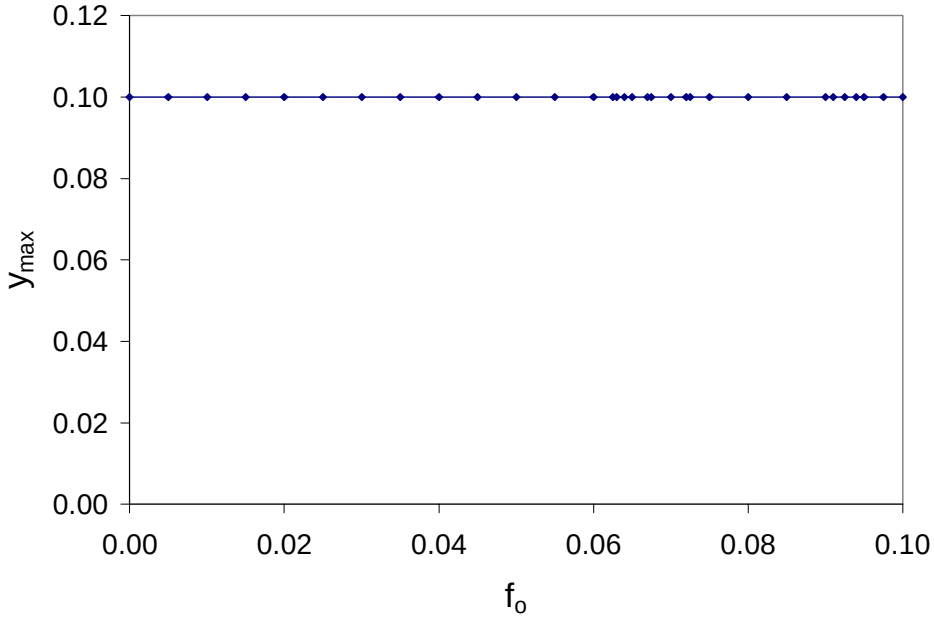

Fig. 6.36. y_{max} vs. f_o, Norm Plot (r=2.5)

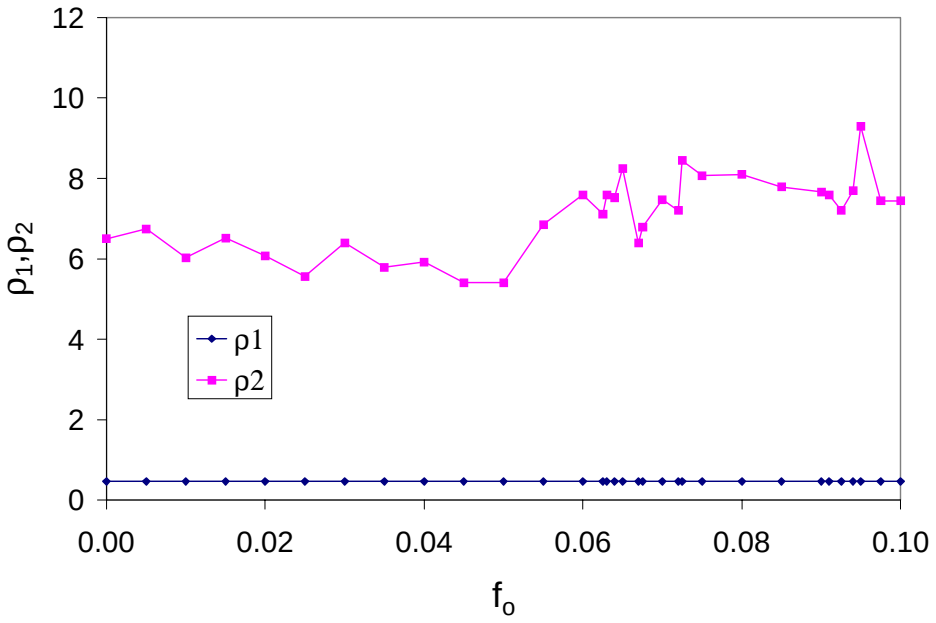

Fig. 6.37. ρ_1 and ρ_2 vs. f_o, Norm Plot (r=2.5)

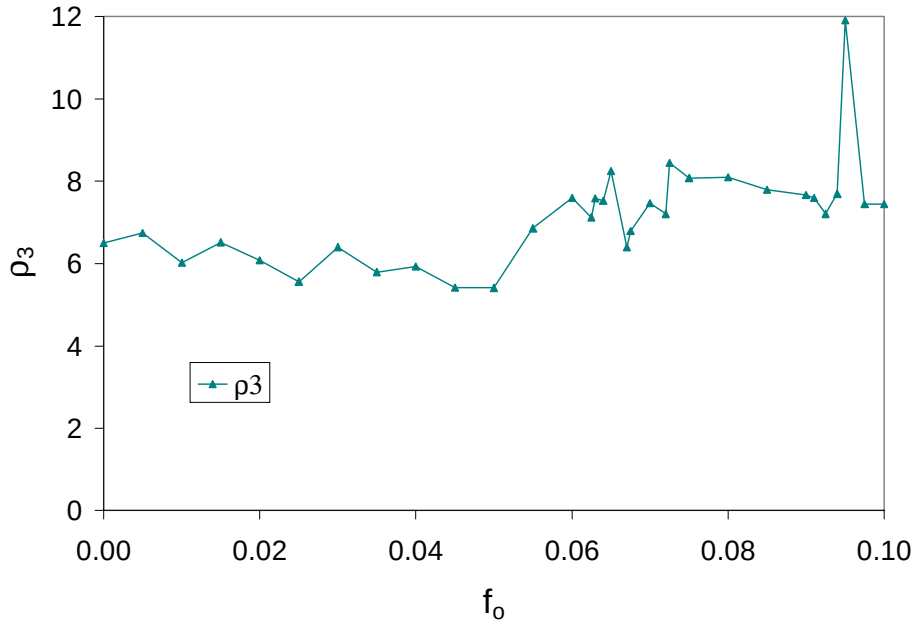

Fig. 6.38. ρ_3 vs. f_o, Norm Plot (r=2.5)

6.5 Special Cases

During the analyses discussed previously, it was found that the RBBW exhibits three types of motion. These motions include slack motions where the RBBW moves about the region with both cables taut. Another motion noticed is referred to as "sliding" motion where the breakwater may slide down a boundary with one cable staying taut. There is also a motion referred to as "rocking" where both cables stay taut and the breakwater simply rocks back and forth near the bottom of the region. These motions were found to exist separately, but also combinations of motions may act together during a solution. For example, a breakwater may be going through slack motions and then the wave forcing pushes it against a boundary and it slides to the bottom of the region. Then it may begin to rock at the bottom and then come out of rocking and slide up a boundary and then come off into a slack motion. It is very possible to have a combination of several of these motions occurring in one solution case. An example of this may be seen in the following sections. The slack motions have been discussed in detail throughout this thesis, and now the two new special motions will be investigated. These two special cases are more likely to occur in nature than the other special cases investigated in Section 4.5.

6.5.1 Sliding Case

A special case that was investigated was a situation when one cable stays taut for some period of time while the other is slack, causing the breakwater to "slide" along a boundary. This situation may be caused by the elliptical wave motions pushing a breakwater into a boundary, along with the normal velocity not being large enough to cause the breakwater to rebound. The breakwater may stay on the boundary (i.e., slide along the boundary) until the wave forcing reverses direction, thus stopping the breakwater from being pushed into the boundary. In the slack motion solution, this type of motion is not accounted for, only a situation where the breakwater instantaneously hits

and rebounds off of a boundary. Thus, the previous solution is no longer valid. Therefore, a special solution for this sliding motion will now be formulated.

6.5.1.1 Sliding Case Formulation

The motions of the sliding motion case resemble that of a double pendulum. The double pendulum motions arise from a cable becoming taut and acting like the upper leg of the pendulum, with the rigid-body breakwater making up the lower leg of the double pendulum. This may be seen in Figs. 6.39 and 6.40. Meirovitch (1970) discusses the motions of a double pendulum in terms of Lagrange's Equations. Thus, the formulation of the sliding motion situation for any RBBW shape may be derived using geometry and Meirovitch's double pendulum formulation. The geometry for the $g_1=0$ and $g_2=0$ boundaries respectively may be seen in Figs. 5.4 and 5.5, where the dimensions are in terms of x and y, and the corresponding geometry where the dimensions are in terms of angles α and β may be seen in Figs. 6.39 and 6.40.

The derivation of the left cable being taut and the breakwater sliding along the $g_2=0$ (right boundary) boundary will be developed first. From the geometry of $g_2=0$ and $g_1<0$, seen in Fig. 6.40, the following relationships may be derived in terms of the rotation angles α and β:

$$x = r\sin\alpha + a\sin\beta - b\cos\beta - 1 \tag{6.5}$$

$$\dot{x} = r\dot{\alpha}\cos\alpha + a\dot{\beta}\cos\beta + b\dot{\beta}\sin\beta \tag{6.6}$$

$$y = h + b - r\cos\alpha - a\cos\beta - b\sin\beta \tag{6.7}$$

$$\dot{y} = r\dot{\alpha}\sin\alpha + a\dot{\beta}\sin\beta - b\dot{\beta}\cos\beta \tag{6.8}$$

$$\theta = \beta - \frac{\pi}{2} \tag{6.9}$$

$$\dot{\theta} = \dot{\beta} \tag{6.10}$$

Rearranging these equations, one can get α, $\dot{\alpha}$, β, and $\dot{\beta}$ in terms of x, $\dot{x}$, y, $\dot{y}$, θ, and $\dot{\theta}$:

$$\alpha = \arcsin\left[(1 + x - a\cos\theta - b\sin\theta)/r\right] \tag{6.11}$$

$$\dot{\alpha} = \frac{\dot{x} + a\dot{\theta}\sin\theta - b\dot{\theta}\cos\theta}{h + b - y + a\sin\theta - b\cos\theta} \tag{6.12}$$

$$\beta = \frac{\pi}{2} + \theta \tag{6.13}$$

$$\dot{\beta} = \dot{\theta} \tag{6.14}$$

Equations 6.11 through 6.14 give the initial conditions for sliding in terms of angles α and β. To get the equations of motion (EOM's) in terms of the angles α and β, we use Lagrange's Equations:

$$L = KE - PE \tag{6.15}$$

$$\frac{d}{dt}\left(\frac{\partial L}{\partial \dot{q}}\right) - \frac{\partial L}{\partial q} = Q_q \tag{6.16}$$

where the coordinate q represents α or β here and Q_q is a generalized force (here a moment corresponding to α or β). The kinetic energy of the system comes from rigid-body dynamics and is as follows:

$$KE = \tfrac{1}{2}m\left(\dot{x}^2 + \dot{y}^2\right) + \tfrac{1}{2}I_c\dot{\theta}^2 \tag{6.17}$$

After substituting in the equations for $\dot{x}$, $\dot{y}$, and $\dot{\theta}$ which are in terms of α and β,

$$KE = \tfrac{1}{2}\left[r^2\dot{\alpha}^2 + \left(I_c + a^2 + b^2\right)\dot{\beta}^2 + 2ra\dot{\alpha}\dot{\beta}\cos(\beta - \alpha) + 2rb\dot{\alpha}\dot{\beta}\sin(\beta - \alpha)\right] \tag{6.18}$$

The potential energy of the system comes from the breakwater's height and is as follows:

$$PE = mgy \tag{6.19}$$

After substituting in the equation for y which is in terms of α and β, and since nondimensionalization replaces mg by 1,

$$PE = h - r\cos\alpha - a\cos\beta - b\sin\beta \tag{6.20}$$

By substituting Equations 6.18 and 6.20 into Equation 6.15, the Lagrangian is developed. Specializing Equation 6.16 for the situation being investigated, the following equation is developed:

$$\frac{d}{dt}\left(\frac{\partial KE}{\partial \dot{q}}\right) - \frac{\partial KE}{\partial q} + \frac{\partial PE}{\partial q} = Q_q \tag{6.21}$$

By the use of the principle of virtual work, the values of Q_α and Q_β may be derived:

$$\delta W = Q_\alpha \delta\alpha + Q_\beta \delta\beta \tag{6.22}$$

Figure 6.41 shows how the forces and the displacements are arranged about the taut cable and RBBW. This gives the virtual work done by the forces as

$$\delta W = f_x \delta x + f_y \delta y \tag{6.23}$$

From Equations 6.5 and 6.7, the virtual displacements δx and δy may be written as

$$\delta x = r\cos\alpha \quad \delta\alpha + a\cos\beta \quad \delta\beta + b\sin\beta \quad \delta\beta \tag{6.24}$$

$$\delta y = r\sin\alpha \quad \delta\alpha + a\sin\beta \quad \delta\beta - b\cos\beta \quad \delta\beta \tag{6.25}$$

The nondimensional values of f_x and f_y may be seen in Equations 4.14 and 4.16, respectively.

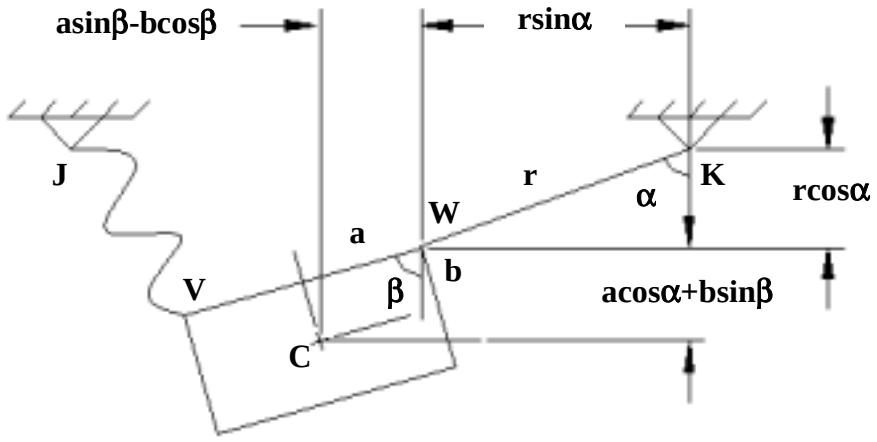

Fig. 6.39. Right Cable Taut with Dimensions in Terms of α and β

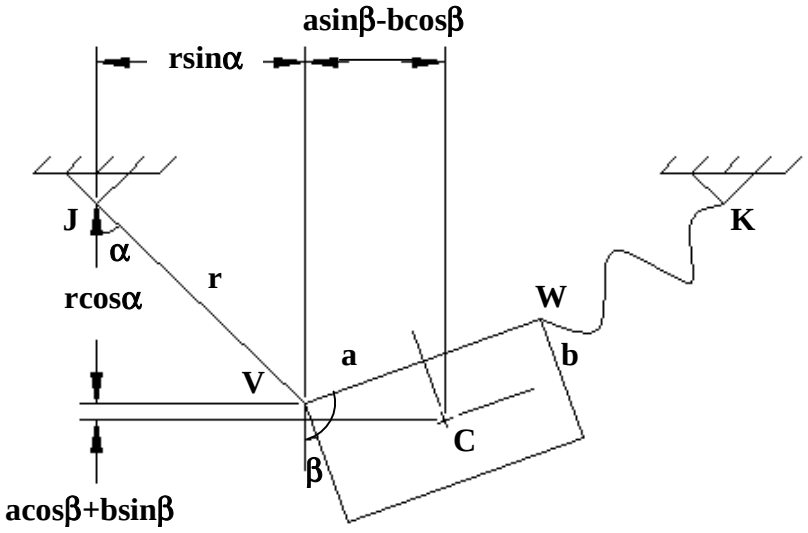

Fig. 6.40. Left Cable Taut with Dimensions in Terms of α and β

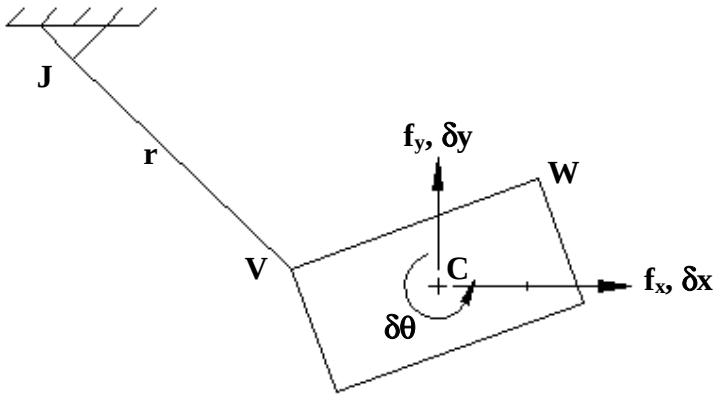

Fig. 6.41. Left Cable Taut with Forces and Virtual Displacements Shown

By plugging Equations 6.24 and 6.25 into Equation 6.23 and then by simplifying, rearranging, and comparing to Equation 6.22, the values of Q_α and Q_β are as follows:

$$Q_\alpha = f_x r\cos\alpha + f_y r\sin\alpha \tag{6.26}$$

$$Q_\beta = f_x(a\cos\beta + b\sin\beta) + f_y(a\sin\beta - b\cos\beta) \tag{6.27}$$

By using Equations 6.18, 6.20, 6.26, and 6.27 in Lagrange's Equations (Equation 6.21) and then by rearranging and grouping the terms, the following generalized equations are obtained:

$$a_{11}\ddot{\alpha} + a_{12}\ddot{\beta} = B_1 \tag{6.28}$$

$$a_{21}\ddot{\alpha} + a_{22}\ddot{\beta} = B_2 \tag{6.29}$$

where

$$a_{11} = r^2 \tag{6.30}$$

$$a_{12} = ra\cos(\beta - \alpha) + rb\sin(\beta - \alpha) \tag{6.31}$$

$$a_{21} = a_{12} \tag{6.32}$$

$$a_{22} = I_c + a^2 + b^2 \tag{6.33}$$

$$B_1 = ra\dot{\beta}^2\sin(\beta - \alpha) - rb\dot{\beta}^2\cos(\beta - \alpha) - r\sin\alpha + Q_\alpha \tag{6.34}$$

$$B_2 = -ra\dot{\alpha}^2\sin(\beta - \alpha) + rb\dot{\alpha}^2\cos(\beta - \alpha) - a\sin\beta + Q_\beta \tag{6.35}$$

By using Cramer's Rule, the values of $\ddot{\alpha}$ and $\ddot{\beta}$ may be determined. However, a numerical technique was needed to solve the equations. A program written in FORTRAN was used to obtain the solution of these ordinary differential equations (ODE's). The DIVPAG subroutine from IMSL was applied. DIVPAG requires the ODE's to be in first-order form. The solutions were used to obtain the x, $\dot{x}$, y, $\dot{y}$, θ, and $\dot{\theta}$ values from Equations 6.5-6.10.

This solution is valid as long as the left cable is in tension (i.e., taut). Therefore, a formulation is required so that it is known when the cable loses tension. This formulation will also use Lagrange's Equations, but now the constraint of $g_2=0$ will be imposed on this solution and will be in terms of x, y, and θ where these terms are equal to q. This idea may be seen in Meirovitch (1970), and the solution is as follows:

$$\frac{d}{dt}\left(\frac{\partial L}{\partial \dot{q}}\right)-\frac{\partial L}{\partial q}=Q_q+\lambda\frac{\partial g_2}{\partial q} \tag{6.36}$$

Using Equations 5.37, 6.18, and 6.20, and the generalized forces

$$Q_x=f_x \tag{6.37}$$

$$Q_y=f_y \tag{6.38}$$

$$Q_\theta=0 \tag{6.39}$$

the following equations are obtained:

$$\ddot{x}=f_x+\frac{2\lambda(1+x-a\cos\theta-b\sin\theta)r}{r} \tag{6.40}$$

$$\ddot{y}=f_y-1+\frac{2\lambda(y-h-b-a\sin\theta+b\cos\theta)r}{r} \tag{6.41}$$

$$I_c\ddot{\theta}=2\lambda\left[(1+x)(a\sin\theta-b\cos\theta)+(h+b-y)(a\cos\theta+b\sin\theta)\right] \tag{6.42}$$

where λ is known as the Lagrange multiplier. Interpreting Equations 6.40 and 6.41, it is found that the axial compression in the cable is 2λr. Thus, when the cable goes into compression (i.e., loses tension), the above solution is no longer valid and the analytical solution for no sliding should resume. For this to occur, λ>0. Then, using Equations 6.5, 6.7, and 6.9, one can write Equation 6.42 in terms of α and β:

$$I_c\ddot{\beta}=2\lambda r\left[a\sin(\beta-\alpha)-b\cos(\beta-\alpha)\right] \tag{6.43}$$

Thus, sliding will stop when the cable loses tension (λ>0) and this will happen when the following condition arises:

$$\ddot{\beta}\left[a\sin(\beta-\alpha)-b\cos(\beta-\alpha)\right]>0 \tag{6.44}$$

A similar derivation for the case where the right cable is taut and the breakwater is sliding along the $g_1=0$ (left boundary) boundary may be performed. The geometry of $g_1=0$ and $g_2<0$ may be seen in Fig. 6.39. Thus the fundamental equations in this derivation are as follows:

$$x = 1 - r\sin\alpha - a\sin\beta + b\cos\beta \tag{6.45}$$

$$\dot{x} = -r\dot{\alpha}\cos\alpha - a\dot{\beta}\cos\beta - b\dot{\beta}\sin\beta \tag{6.46}$$

$$y = h + b - r\cos\alpha - a\cos\beta - b\sin\beta \tag{6.47}$$

$$\dot{y} = r\dot{\alpha}\sin\alpha + a\dot{\beta}\sin\beta - b\dot{\beta}\cos\beta \tag{6.48}$$

$$\theta = \frac{\pi}{2} - \beta \tag{6.49}$$

$$\dot{\theta} = -\dot{\beta} \tag{6.50}$$

Rearranging these equations, one can get α, $\dot{\alpha}$, β, and $\dot{\beta}$ in terms of x, $\dot{x}$, y, $\dot{y}$, θ, and $\dot{\theta}$:

$$\alpha = \arcsin\left[(1 - x - a\cos\theta + b\sin\theta)/r\right] \tag{6.51}$$

$$\dot{\alpha} = \frac{\dot{x} - a\dot{\theta}\sin\theta - b\dot{\theta}\cos\theta}{y - h - b + a\sin\theta + b\cos\theta} \tag{6.52}$$

$$\beta = \frac{\pi}{2} - \theta \tag{6.53}$$

$$\dot{\beta} = -\dot{\theta} \tag{6.54}$$

From a similar virtual work derivation as before,

$$Q_\alpha = -f_x r\cos\alpha + f_y r\sin\alpha \tag{6.55}$$

$$Q_\beta = -f_x(a\cos\beta + b\sin\beta) + f_y(a\sin\beta - b\cos\beta) \tag{6.56}$$

The solution procedure discussed above for the values of α, $\dot{\alpha}$, β, and $\dot{\beta}$ is the same for this derivation with Equations 6.55 and 6.56 replacing Equations 6.26 and 6.27 (i.e., the sign in front of f_x changes). This solution is valid as long as Equation 6.44 is satisfied.

Both of the sliding solutions discussed above are valid as long as a cable is under tension, and when tension is lost the solution reverts back to the previous slack condition solution. However, the situation may arise where the breakwater slides down a boundary and strikes the origin, thus making both cables taut. This situation is handled by using the initial conditions from the sliding case and applying these values to the normal impact equations discussed in Section 5.5.

6.5.1.2 Sliding Case Results

During the analysis of this problem, some of the cases analyzed would go into a sliding condition and would stay on a boundary for some period of time. This motion can not be handled by the previously used analytical solution, thus the numerical solution above was developed to handle this situation because it would not be accurate to simply stop the analysis if this motion would occur. When a RBBW goes into a sliding motion, the breakwater may slide either up a boundary, down a boundary, or simply rotate about a connection point while one cable is taut, essentially rotating the center of the breakwater into the region. All three of these motions were seen in the example discussed later. Since none of the solutions analyzed in Table 6.1 exhibited the special motion of sliding, some cases where this motion occurred were found from several additional analyses performed. Because of the large number of analyses conducted, not all will be shown; only an example which best depicts the behavior of a RBBW undergoing sliding will be illustrated, but the conclusions were drawn from all analyses.

It was found through many analyses that there is no set pattern to predict what parameters and initial conditions would cause a RBBW to go into a sliding condition. Sliding occurred for all of the RBBW shapes, for both radii, and at various parameters and conditions used throughout this investigation. Thus, no conclusion can be drawn as to why a breakwater would go into sliding in one case but not another. The only way to say that a breakwater would slide is when the normal velocity is very low, and this can not be

determined prior to an analysis being conducted. The highly nonlinear nature of the problem plays a major role in the occurrence of sliding.

Looking at the physical application of the problem to an actual breakwater in the sea, one can imagine that any shape, size, or configuration of a floating moored object might feel this sliding effect at some time during its life. Further, any one of the many variables involved in this type of problem might lead to a sliding condition. As seen in Fig. 6.42, if waves are pushing a breakwater in one direction long enough, one cable may be slack while the other is taut for a period of time. This might result from waves coming into the breakwater at a very high frequency and the breakwater may not be able to respond in an opposite direction. This might also be true if a very large breakwater is absorbing a lot of waves because of its size. These are just two examples of how any number of conditions might lead to a breakwater sliding (i.e., one cable being taut) and this can not be predicted.

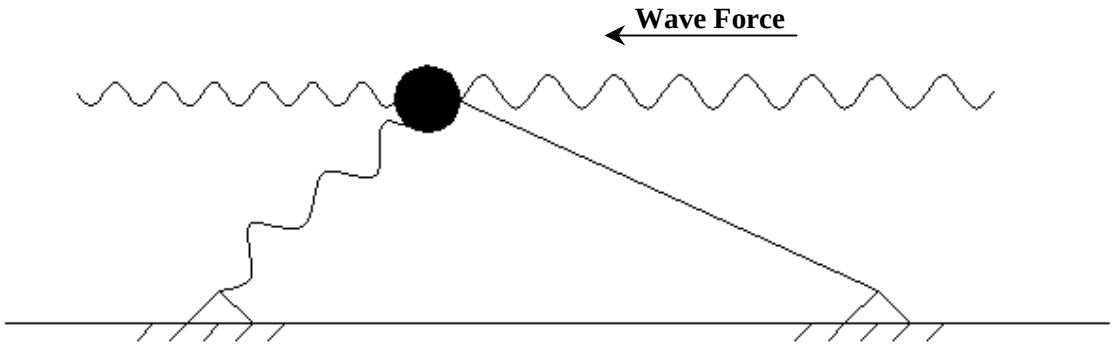

Fig. 6.42. Breakwater with One Cable Taut (Sliding) Being Pushed by Waves

The following is an example of one of the many cases where the sliding motion occurred sometime during the motion of the RBBW. The parameters and initial conditions used to produce this case are as follows:

$r=1.5$ $e=0.9$

$a=0.1$ $b=0.0$

$x(0)=0.0$ $y(0)=0.1$ $\theta(0)=0.0$ (6.57)

$\dot{x}(0) = 0.0$ $\dot{y}(0) = 0.0$ $\dot{\theta}(0) = 0.0$

$f_o=0.27$ $\nu=0.5$ $\Omega=0.9$

This case exhibited sliding where the RBBW would slide down a boundary with one cable taut until it reached a point where both cables became taut, and then it rebounded back up a boundary (Fig. 6.43). The situation where a RBBW would impact the opposite boundary with one cable already taut (i.e., $g_1=g_2=0$) was handled by simply using the convergence part of the solution method to converge to the time where the breakwater would impact the other boundary. After this impact, using the standard impact conditions, the breakwater would rebound back up off of the opposite boundary and would continue to slide. While sliding back up the boundary, the RBBW would switch direction and travel back down the boundary again. This switching of direction may be caused by gravity taking over the motions, or the elliptical wave forcing switching direction but keeping the RBBW pushed into the boundary. Essentially, the RBBW bounced up and down with one cable taut. The RBBW in this case did not settle to an equilibrium state. Instead, an interesting situation arose where the RBBW rotates about the connection point defining the boundary of which it is sliding. This would bring the center of the RBBW and the other boundary into the region until the breakwater reaches a condition where it is on both boundaries (i.e., both cables taut), and the RBBW begins to rock and the sliding ceases. Point R in Fig. 6.43 denotes where this occurs in the trajectory. Figure 6.43 shows the trajectory of motion for the example case investigated. Like the point R, other important points of the case are noted on the plot. The starting point is indicated with an I. The point where sliding starts is denoted with an S. One of

the many points where the breakwater reaches a point where $g_1=0$ and $g_2=0$ and rebounds off of one boundary is denoted by G. Finally, the point where the RBBW would normally settle to an equilibrium state is denoted with an E. It should be noted that the sliding in this case starts on the left side and then moves to the right side while the RBBW is sliding down the $g_2=0$ boundary (normally on the right side). This is because the boundaries are not definite as in the PMBW problems and the rotations of the RBBW make it possible to have a region for a boundary where the $g_1=0$ and $g_2=0$ could overlap, as seen in this case. The cases investigated would stop sliding by settling to the bottom of the region, reaching the rotation limit, or starting to rock. This example started to rock, and thus the rocking situation will now be described.

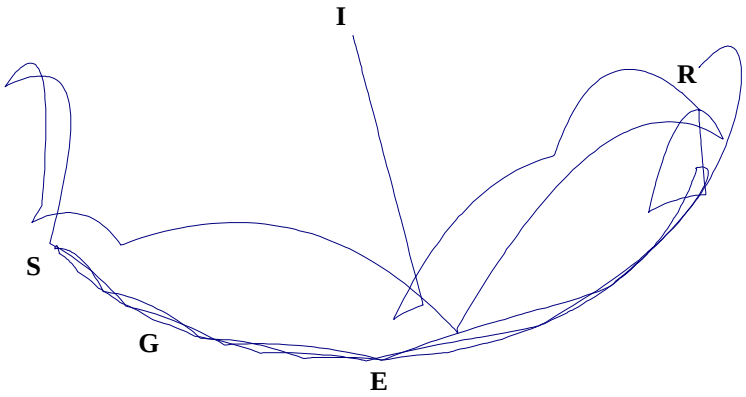

Fig. 6.43. y vs.x, Case 1910001000-2759, Plot Showing Sliding

6.5.2 Rocking Case

Rocking is another special motion seen in the rigid-body breakwater under wave forcing. A rocking situation may occur if the motions of the RBBW settle to the bottom of the region and the wave forcing is not influential enough to carry the breakwater out of this condition. In other words, the rocking case is simple in that if the wave forcing influence is small enough, the breakwater may not become excited enough to have one of its cables lose tension and it may simply rock (i.e., both cables stay taut and the breakwater rocks back and forth). This situation makes an interesting problem for investigation. A mathematical formulation was derived to model the motions of the RBBW while both cables were taut and the breakwater is rocking. This formulation uses the initial data from an analyzed case where the RBBW goes into a rocking condition during the analysis. The rocking formulation describes the motion and conditions where the RBBW comes out of rocking if in fact it does before settling to an equilibrium state. The formulation of the case where b=0 (i.e., the circular shape) will be derived because it is this shape in which this investigation is most interested. Also, the mathematics involved in the case where b≠0 become extremely complex and are not practical to solve for this investigation.

6.5.2.1 Rocking Case Formulation

In the analysis of the RBBW under free motions, when a condition where rocking was probable (i.e., $g_1=g_2=0$ and $y\neq0$), it was assumed that the breakwater would settle to the bottom of the region in a short period of time. This assumption may not be true for the RBBW under forced motions. This is because, unlike the free motion problem where the only force acting on the RBBW was gravity, the present problem being investigated has an elliptical force acting on the RBBW which may pull the breakwater out of an equilibrium state after some rocking. Thus, it is important to have a method to solve this type of condition if this situation arises.

Similar to the derivation of the sliding case, Lagrange's Equations will be used in this derivation to describe the motions of the RBBW during a rocking situation. The configuration for the rocking situation may be seen in Fig. 6.44. This configuration shows the geometry for a situation where g_1=0 and g_2=0 and where the dimensions are in terms of x, y, and θ. Thus, the formulation of the rocking motion situation for a circular RBBW shape may be derived using geometry, seen in Fig. 6.44, and Lagrange's Equations.

With b=0 in this special case, the boundary condition equations become

$$g_1 = (1 - x - a\cos\theta)^2 + (h - y - a\sin\theta)^2 - r^2 = 0 \tag{6.59}$$

$$g_2 = (1 + x - a\cos\theta)^2 + (h - y + a\sin\theta)^2 - r^2 = 0 \tag{6.60}$$

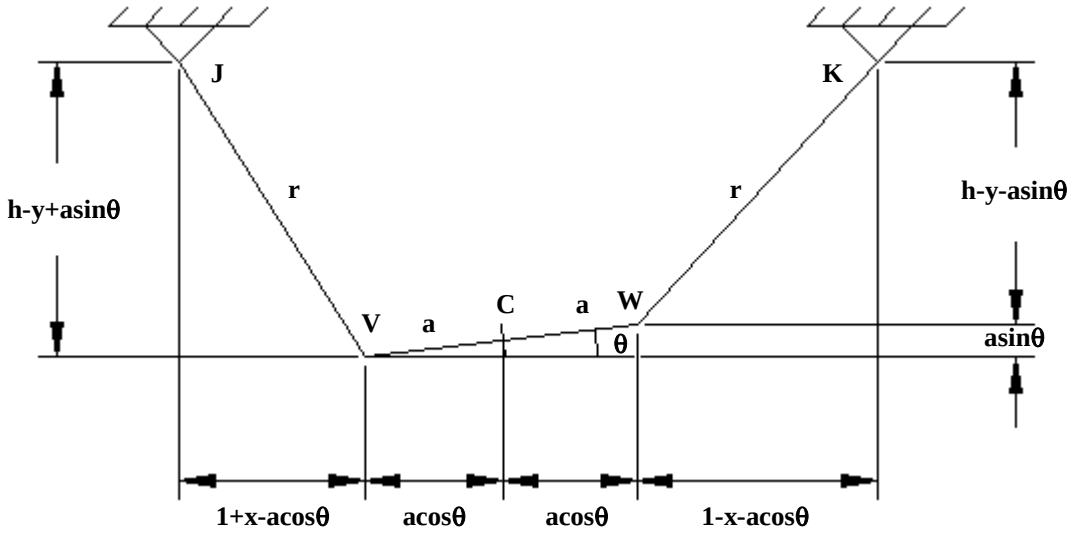

Fig. 6.44. Circular RBBW Rocking Configuration

By examining these equations, it may be seen that the problem really has only one degree of freedom. Thus, x and y can be written in terms of θ. Expanding g_1 and g_2 and then subtracting these equations from one another, the following expression for x in terms of y and θ is obtained:

$$x = \frac{(y-h)a\sin\theta}{(1-a\cos\theta)} \tag{6.61}$$

By expanding and adding Equations 6.59 and 6.60, and using Equation 6.61, the following expression for y in terms of θ is obtained:

$$y = h + \frac{(a\cos\theta - 1)\sqrt{r^2 - 1 - a^2 + 2a\cos\theta}}{\sqrt{1 + a^2 - 2a\cos\theta}} \tag{6.62}$$

The y value in Equation 6.61 may be replaced by Equation 6.62 to give x in terms of only θ. With the x and y equations in terms of θ, Equation 6.16 becomes

$$\frac{d}{dt}\left(\frac{\partial L}{\partial \dot{\theta}}\right) - \frac{\partial L}{\partial \theta} = Q_\theta \tag{6.63}$$

From the principle of virtual work, the following generalized force equation may be developed:

$$\delta W = Q_\theta \delta\theta = f_x \delta x + f_y \delta y + f_\theta \delta\theta \tag{6.64}$$

However, since there is no applied moment, the value of $f_\theta \delta\theta = 0$ and the differential form of Equation 6.64 becomes

$$Q_\theta = f_x \frac{dx}{d\theta} + f_y \frac{dy}{d\theta} \tag{6.65}$$

The generalized force (Equation 6.65) for Equation 6.63 may be developed from Equations 4.14, 4.16, 6.61, and 6.62. Equations 6.17 and 6.19 give the kinetic and potential energies, respectively, for the Lagrangian of Equation 6.15 also to be used in Equation 6.63. This Lagrange Equation leads to an expression for $\ddot{\theta}$ as a function of θ and $\dot{\theta}$. Again, a numerical technique was needed to solve the equations. A program written in FORTRAN was used to obtain the solution of this ordinary differential

equation (ODE). The DIVPAG subroutine from IMSL was applied. DIVPAG requires the ODE to be in first-order form. The solutions were used to obtain the new values of x, $\dot{x}$, y, $\dot{y}$, θ, and $\dot{\theta}$ for the next analysis.

In order to derive the condition for both cables to be taut, the following equations are developed from Lagrange's Equations in terms of x, y, and θ:

$$\ddot{x} = f_x + 2\lambda_1(-1 + x + a\cos\theta) + 2\lambda_2(1 + x - a\cos\theta) \tag{6.66}$$

$$\ddot{y} = f_y - 1 + 2\lambda_1(y - h + a\sin\theta) + 2\lambda_2(y - h - a\sin\theta) \tag{6.67}$$

$$I_c\ddot{\theta} = 2\lambda_1 a[(1-x)\sin\theta - (h-y)\cos\theta] + 2\lambda_2 a[(1+x)\sin\theta + (h-y)\cos\theta] \tag{6.68}$$

where λ_1 and λ_2 are Lagrange multipliers and are dependent upon time. Interpreting Equations 6.66 and 6.67, it is found that the axial compression in the right cable is $2\lambda_1 r$ and the axial compression in the left cable is $2\lambda_2 r$. To determine if the RBBW is still in a rocking condition, the differential equations above (Equations 6.66-6.68) need to be solved with the algebraic equations for $g_1=0$ and $g_2=0$ (Equations 6.59 and 6.60, respectively) for x(t), y(t), θ(t), $\lambda_1(t)$, and $\lambda_2(t)$. When one or both cables go into compression (i.e., lose tension), the above solution is no longer valid. There are three situations in which this may occur. If $\lambda_1>0$ and $\lambda_2>0$, (i.e., both cables slack) then the analytical solution should be applied. If either $\lambda_1>0$ and $\lambda_2<0$ (i.e., right cable slack) or $\lambda_1<0$ and $\lambda_2>0$ (i.e., left cable slack), then the sliding solution should be applied.

6.5.2.2 Rocking Case Results

A rocking situation usually results when an analyzed case dissipates enough energy to cause the RBBW to not be able to get out of a region near the equilibrium state because gravity has pulled the breakwater near this state. While near the bottom of the region, the mooring lines of the RBBW may become taut for a period of time while the breakwater is rotating back and forth (i.e., rocking) due to its rotational ability. However, the RBBW may not settle to an equilibrium state in this problem. The RBBW may gain the ability to

climb out of a rocking situation and start sliding up one boundary or go back into a fully slack condition. This is because the RBBW is undergoing directional elliptical wave forcing. Either of these situations made it necessary to develop the above formulation in order to see if a RBBW indeed attains equilibrium or comes out of rocking.

Picking up where the case in Section 6.5.1.2 left off, the rest of the situation of that example will now be discussed. In that case the rocking only lasted a short period of time before one cable lost tension and the breakwater began to slide again. After the second sliding occurred, the breakwater settled to the bottom of the region. This is an example of where the RBBW comes out of rocking before settling to the bottom of the region. Now a case where the RBBW settles to an equilibrium state will be investigated. The parameters and initial conditions used to produce this case are as follows:

$r=1.5$	$e=0.9$		
$a=0.1$	$b=0.0$		
$x(0)=0.0$	$y(0)=0.1$	$\theta(0)=0.0$	(6.69)
$\dot{x}(0) = 0.0$	$\dot{y}(0) = 0.0$	$\dot{\theta}(0) = 0.0$	
$f_o=0.1$	$\nu=0.5$	$\Omega=0.9$	

This case exhibited rocking where the RBBW would stay near the equilibrium state for a period of time with both cables being taut (i.e., $g_1=g_2=0$). Figure 6.45 shows the trajectory of motion for the example case investigated. This case is a continuation of the analytical solution of the case 1910001000-159 in Table 6.1. After the motions start to die out during the solution of the case, the RBBW does not have enough energy to rebound off of the boundaries. Further, since the forcing is low and the fact that the RBBW reaches a position where g_1 and g_2 are practically zero, the rocking solution is applicable. Once the RBBW enters rocking, the influence of the wave forcing is not significant enough for the RBBW to come off of the boundaries. Once in this situation, the horizontal component of the wave forcing takes control of the motions and continuously pushes the breakwater in a rocking motion. As before, some important points are noted on Fig. 6.45. The starting point is indicated with an I. Point R denotes

the point where rocking begins. The point where the RBBW settles near the equilibrium state is denoted with an E. It may be noticed in this figure that the region where the impact boundaries can exist may be seen. This region lies between the sharp points of the trajectory plot, which show where one cable becomes taut and the RBBW rebounds off of a boundary and the circular arc formed by both cables being taut and the breakwater rocking. The sharp points are above the circular arc formed by the rocking situation, indicating that the RBBW must have been rotated when it struck the boundary. If it were rotated perfectly in alignment with the boundary then, it would produce a point very close to the circular arc. The nice circular arc of the rocking shows that when both cables are taut, the only variable affecting the boundary is the rotation and the arc is formed from the breakwater being in its lowest region with θ changing. Thus, a region where boundaries can exist extends from a rotated RBBW with one cable taut situation to a situation where both cables are taut and the RBBW is rotating (rocking).

Thus, rocking may occur in two different manners and may end in two different manners as well. Rocking may begin when a RBBW is sliding and then hits the opposite boundary; if the breakwater does not have enough energy to get back off of the boundary, it would begin rocking. Another instance where rocking may begin is when a RBBW settles to the bottom of the region and does not have enough energy to get out of this settling and the breakwater starts to rock at the bottom of the region. Rocking may end if the situation arises that the elliptical wave forcing can pull the RBBW free from the rocking. After the breakwater is freed it may start to slide again or go into the slack region. Ultimately, the final stopping of the rocking condition would be if the RBBW would simply settle and end up in the equilibrium state. Rocking may occur in almost any case where the conditions are right, but the forcing amplitude has a significant effect on whether and for how long rocking will occur. The lower the value of f_o, the more likely the breakwater will stay in a rocking condition. Whatever the manner by which a RBBW starts to rock or stops rocking, the situation where rocking occurs during the motions of a RBBW is significant and therefore has been analyzed.

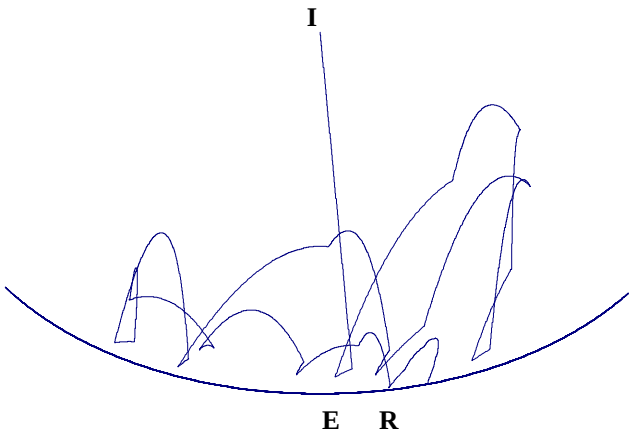

Fig. 6.45. y vs.x, Case 1910001000-159, Plot Showing Rocking